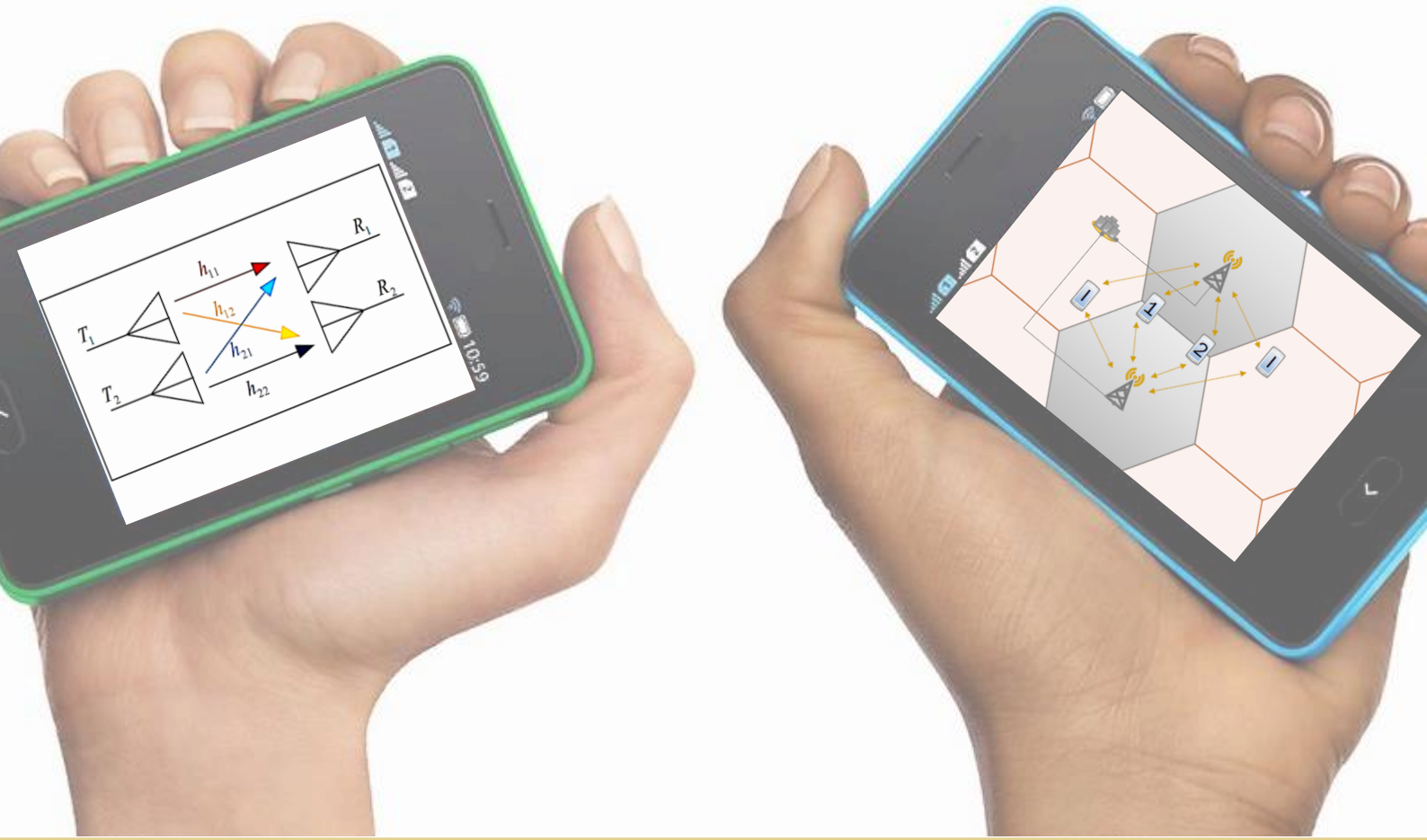

João Francisco Cardoso Gante

IB-DFE Techniques Applied to Multi-Antenna Systems

Setembro de 2014

· U C ·

Universidade de Coimbra

IB-DFE Techniques Applied to Multi-Antenna Systems

João Francisco Cardoso Gante

Dissertação para obtenção do Grau de Mestre em

Engenharia Electrotécnica e de Computadores

Orientador:	Doutor Marco Alexandre Cravo Gomes
Co-Orientador:	Doutor Vítor Manuel Mendes da Silva

Júri

Presidente:	Doutor Luís Alberto da Silva Cruz
Orientador:	Doutor Marco Alexandre Cravo Gomes
Vogais:	Doutora Lúcia Maria dos Reis Albuquerque Martins
	Doutor Rui Miguel Henriques Dias Morgado Dinis

Setembro de 2014

Agradecimentos

Em primeiro lugar, gostaria de agradecer ao professor Marco Gomes, ao professor Vítor Silva e ao professor Rui Dinis, não só pela possibilidade de ter participado neste projeto, mas também pelos preciosos ensinamentos dados no decorrer do trabalho para esta dissertação.

Aos meus pais e à minha irmã, cujo empenho desde o primeiro dia da minha existência permitiu que eu conseguisse atingir os meus objetivos, e ao qual estou eternamente grato.

Aos meus colegas de laboratório, pelo ótimo ambiente de trabalho proporcionado. Para além das inúmeras dúvidas esclarecidas, sem eles o relógio desde último ano teria avançado lentamente.

Por último, mas não de todo menos importante, à Joana Pereira, cuja complexidade torna uma dissertação de mestrado num mero quebra-cabeças para crianças. Obrigado por desafiares o modo como vejo o mundo, dia após dia, e por me ajudares a seguir os meus sonhos, mesmo os mais irrealistas.

A todos os que me apoiaram, pela sua paciência e dedicação,

Muito Obrigado.

Abstract

With the rise of data-hungry mobile services, scientists have struggled to deliver the desired mobile data rates whilst using the limited available bandwidth. As the higher frequencies are yet inaccessible, namely the millimeter wave frequencies (between 60 and 100 GHz), spectral efficiency is becoming the defining factor for future standards. As result of this, MIMO techniques have been gathering interest in the past few years. The basic concept of a MIMO system consists in transmitting different signals through several antennas, using the same frequency band and with at least as many receiving antennas on the receiver. Exploiting the lack of correlation between the multiple channels, it is possible to isolate and detach each received signal at the receiver. While it seems to be a straightforward method to increase the spectral efficiency, as result of multiple signals being squeezed in the same frequency band, the complexity of the signal separation algorithms is awfully high. Additionally, these algorithms fail to separate signals whose power is far inferior than their peers', imposing limitations to MIMO based systems. This work proposes three independent solutions to improve MIMO uplink communications for single-carrier block-based transmissions with iterative frequency domain equalization (IB-DFE). The first uses magnitude modulation techniques so as to improve the transmitter's power efficiency. The second employs base station cooperation techniques to improve the user's performance at cell edges. Lastly, the third solution apply a cluster-based multi-user detection, allowing for an increased number of users to share the same channel without exhausting the computational resources at the receiver.

Keywords

Signal Processing, IB-DFE, MIMO, Base Station Cooperation, Magnitude Modulation, Multi-user Detection

Resumo

Com o aumento exponencial do tráfego de dados por parte dos serviços móveis, a comunidade científica tem tido dificuldades em desenvolver técnicas que permitam atingir a capacidade de transmissão de dados móveis desejada, devido à largura de banda física limitada. Como as bandas de frequências mais elevadas ainda não estão disponíveis para uso, nomeadamente as bandas milimétricas (60 a 100 GHz), a eficiência espectral tem-se tornado um fator chave na escolha das tecnologias adotadas. Como resultado, as técnicas MIMO têm reunido um grande interesse nos últimos anos. O conceito básico de um sistema MIMO consiste em transmitir diferentes sinais através de várias antenas, com recurso à mesma gama de frequências e com tantas ou mais antenas no lado do recetor. Ao tirar partido da falta de correlação entre os múltiplos canais, é possível isolar e extrair cada um dos sinais recebidos no recetor. Apesar de parecer um método simples para aumentar a eficiência espectral, dado que os vários sinais partilham a mesma gama de frequências, os algoritmos de separação dos sinais no recetor têm uma complexidade elevada. Para além do mais, estes algoritmos são ineficazes a extrair sinais cuja potência é consideravelmente inferior à dos seus pares, o que por sua vez impõe algumas limitações na implementação de sistemas MIMO. Esta tese propõe três soluções independentes para melhoria de comunicações MIMO no sentido ascendente (*uplink*), baseadas em sistemas de transmissão de mono-portadora por bloco com equalização iterativa no domínio da frequência (IB-DFE). A primeira solução usa a modulação de magnitude de modo a aumentar a eficiência energética dos transmissores MIMO. A segunda proposta explora a cooperação entre estações base, de modo a melhorar o desempenho dos utilizadores nos limites das células móveis. Por fim, a terceira solução propõe a deteção de múltiplos utilizadores agrupados em diferentes níveis de potência, permitindo que um número superior de utilizadores partilhe o mesmo canal físico.

Palavras-Chave

Processamento de Sinal, IB-DFE, MIMO, Cooperação de Estações Base, Modulação de Magnitude, Deteção de Multi-utilizadores

Contents

List of Figures

List of Tables

List of Acronyms

3G	third generation
4G	fourth generation
5G	fifth generation
AWGN	additive white gaussian noise
BER	bit error rate
BS	base station
CE	cyclic extension
DAC	digital-to-analog converter
DFT	discrete Fourier transform
FD	frequency domain
FDE	frequency domain equalization
HPA	high power amplifier
IB-DFE	iterative block decision feedback equalization
ISI	intersymbol interference
LDPC	low-density parity-check
LTE	long-term evolution
LUT	look-up table
MIMO	multiple-input and multiple-output
MM	magnitude modulation

MPMM	multistage polyphase magnitude modulation
MT	mobile terminal
MU-MIMO	multi-user multiple-input and multiple-output
PAPR	peak-to-average power ratio
PC	polar clipping
PS	polar scaling
QoS	quality of service
QPSK	quadrature phase-shift keying
RC	rectangular clipping
RRC	root-raised cosine
RS	rectangular scaling
SC	single carrier
SIC	successive interference cancellation
SISO	single-input and single-output
SNIR	signal to interference plus noise ratio
SNR	signal-to-noise ratio
TD	time domain

1

Introduction

Contents

Mobile communications data usage has experienced an enormous growth burst in the last few years. The number of smartphones is quickly rising and third generation (3G) networks widely cover most countries, some of which also have faster networks such as long-term evolution (LTE) or LTE advanced (fourth generation (4G)). Recent studies [1] have shown that global mobile data traffic grew 81 percent in 2013 and it is expected to grow sixfold from 2014 until the end of 2018 [1]. Mobile data traffic represents more than half of the total data traffic and 2013's mobile data traffic was nearly 18 times the size of the entire global Internet in 2000. These crushing numbers show that the capacity must be increased, in order to keep (or to improve) the existing mobile communications' quality of service (QoS).

1.1 Motivation

The easiest mean to achieve a higher capacity of a given system, which in turn can lead to a better QoS through better and faster services, would be to increase the used physical bandwidth, as the achievable maximum bit rate is directly proportional to it. However, the available bandwidth is extremely limited, with the higher frequencies not yet occupied being impossible to use as of now. Even though future standards (i.e. the fifth generation (5G)) hope to lift this constraint [2], they won't come up fast enough to be the answer to our society's very short-term needs. The solution to our problem consists then on improving the existing spectral efficiency or, in other words, to squeeze a higher data rate in the same available bandwidth. There are two different means to do so: either the individual communication links are improved or the overall system capacity is upgraded with more links. Unfortunately, the individual link capacities are already close to the fundamental Shannon limit, so, further improvements are mostly restricted to the overall system's capacity [3] [4].

Multiple-input and multiple-output (MIMO) systems are indeed a great answer to the increasing mobile data usage [5] [6]. By allowing more individual links to coexist in the same physical channel, the overall spectral efficiency can increase up to as many times as the minimum between the number of simultaneously transmitted signals and the number of receiving antennas, without increasing the total transmitted power[1] [7]. However, as each receiving antenna contains tangled information regarding all the transmitted signals, a complete recovery of those signals requires signal separation techniques. The signal separation of a MIMO system is a very complex and highly demanding operation. Additionally, it must be executed alongside the equalization (as it will be soon discussed) and,

[1] Alternatively, it is possible to keep the overall spectral efficiency, while decreasing the total transmitted power.

therefore, the equalizer of a MIMO system must be slightly different than single-input and single-output (SISO)'s equalizer [8] [9] [10].

A useful generalization of a MIMO system is the multi-user multiple-input and multiple-output (MU-MIMO) system. While in a MIMO system both communicating sides consist of a single device with multiples antennas, in a MU-MIMO the multiple antennas are spread among several devices [11]. As a MIMO equalizer is oblivious of the signal's origin, the same equalization scheme can be used for both MIMO and MU-MIMO. A clear example of a MU-MIMO would be a telecommunications cell with a base station (BS) connected with several mobile terminals (MTs) through the same physical channel, a system whose overall uplink spectral efficiency gain and computational effort would be the same as if the MTs were a single device with the same total transmitted power [12] [13]. Nevertheless, while a multi-antenna transmitter in a MIMO (or MU-MIMO) can both decrease its total transmitted power and increase its data throughput, a given MT with a single transmitting antenna must keep its transmitted power so as to keep its individual data throughput.

A robust MIMO (or MU-MIMO) equalization is then of utmost importance. It brings forth not only the desired enhanced spectral efficiency, but also allows for a higher transmitting power efficiency for the battery-limited mobile users with multiple antennas, culminating in a better overall mobile communications system.

1.2 Objectives and Main Contributions

After this brief analysis, it became clear how relevant it would be to study uplink MIMO equalization, namely how to increase both power and spectral efficiency. All the proposed changes are applied to the promising iterative block decision feedback equalization (IB-DFE) scheme, aiming to quantify the magnitude improvement on state of the art equalization techniques. For that very reason, the implementation of channel coding is also tested for every scenario.

Regarding the power efficiency, it was applied a magnitude modulation (MM) technique at the MIMO transmitter. As the MM scales down the symbols whose output after pulse shaping filter is higher than a given threshold, the peak-to-average power ratio (PAPR) at each transmitting antenna is restrained. As result, the transmitter's power efficiency was considerably increased, while introducing minimal distortion to the transmitted symbols. This led to one accepted paper on the Vehicular Technology Conference 2014-Fall [14].

To tackle the spectral efficiency issue, situations with base station cooperation and clustering were exploited. By employing base station cooperation schemes, it is possible

to make use of MIMO's channel diversity properties when working with mobile users sharing the same cell edges, greatly reducing the minimum power requirements while increasing the spectral efficiency. Regarding the clustering of users, it is proved that if on a given physical channel there are clusters of users with enough power difference between them at the receiver, it is possible to successfully detect all the users. This method not only gives room for increased spectral efficiency, but also reduces the total computational effort needed. Each one of these techniques lead to a submitted paper, to the Vehicular Technology Conference 2015-Spring [15] and to the International Conference on Communications [16]

1.3 Dissertation Outline

This thesis is organized in five chapters. Succeeding the introduction, Chapter 2 will provide an overview on MIMO and MU-MIMO systems, where its benefits and limitations on the overall communication system are elucidated. Chapter 3 lays emphasis on the IB-DFE scheme, where careful attention is payed to mathematical formulation of the equalizer and its relationship with channel coding. Chapter 4 not only studies the power efficiency improvement at the MIMO transmitter using MM techniques, but also aims to improve the MU-MIMO spectral efficiency through user clustering and BS cooperation. Finally, Chapter 5 discusses the main conclusions drawn from this thesis work.

As a side note, most of the mathematical proofs in chapter 2 are shown in a very summarized manner, so as to enlighten a unacquainted reader about the potentials of those techniques. The mathematical aspects of this chapter are quite extensive and, therefore, if the reader desires to fully understand the matter, it is suggested the reading of the supplied bibliography.

2

MIMO Concepts

Contents

The use of multiple antennas at the transmitter and receiver in wireless systems, known as MIMO technology, has rapidly gained in popularity over the past decade due to its powerful performance-enhancing capabilities. Those performance-enhancing capabilities come from:

- Beamforming gain — the capacity of adding coherently the different transmitted signals at specific locations, so as to simultaneously increase the signal to interference plus noise ratio (SNIR) at the desired receivers while minimizing it for undesired receivers;
- Spatial diversity gain — sending the same signal through several links decreases the probability of that given signal to be critically faded at the receiver;
- Spatial multiplexing gain — it is possible to send different information through different transmitting antennas.

In general, it may not be possible to exploit simultaneously all the benefits described above due to conflicting demands on the spatial degrees of freedom [17]. However, using some combination of the benefits across a wireless network will result in improved capacity, as detailed in the following section.

2.1 Channel Capacity

In 1948, Claude Shannon completed an information theory law left by Ralph Hartley [3]. The resulting Shannon-Hartley theorem, shown in equation (2.1), specifies the maximum bit rate at which information can be transmitted over a single communication channel with a given bandwidth B, as function of the signal-to-noise ratio (SNR). If a given system has a throughput lower than this limit, it can be transmitted with asymptotically small probability of error.

$$C = B\log_2(1+SNR) \tag{2.1}$$

Equation 2.1 proves that a SISO link has a maximum spectral efficiency (C/B) for given SNR. While it is possible to increase the maximum spectral efficiency of the links through extra signal power, mobile devices would have to drain power from their batteries several times faster in order to achieve a considerable gain. As an example, a link whose SNR is of 10dB would need to increase his power tenfold in order to achieve a maximum spectral efficiency almost twice as high, due to the logarithmic nature of the relationship. The solution to boost the real spectral efficiency of a given link without increasing the transmitted power is then restricted to apply techniques such as coding and

signal processing [3], so as to approach as much as possible its maximum theoretical value. However, even that solution is close to its saturation point for several scenarios, as shown in [4].

2.1.1 SISO and MIMO Channel Capacity Comparison

Considering a narrowband frequency flat fading channel without time dispersion, a SISO link can be represented as in Fig. 2.1.

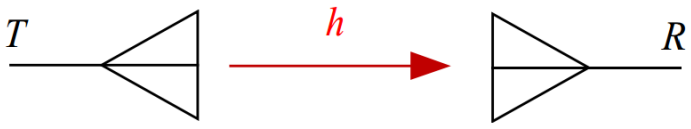

Figure 2.1: Representation of a SISO channel.

Here, the time domain signal at the receiver for a given instant is given by

$$y = hx + n\,, \tag{2.2}$$

where y is the received signal, h is the channel response, x is the transmitted signal and n is the additive white gaussian noise (AWGN) channel noise. Note that it is not a convolution, as the channel has no time dispersion. If the channel response is known, it is easy to obtain an estimation of the transmitted signal through the received signal, dividing y by h. Extending the SISO paradigm, it is clear that to increase capacity, one can just replicate the link T times[1], sending all the information through the same physical channel as shown in Fig. 2.2.

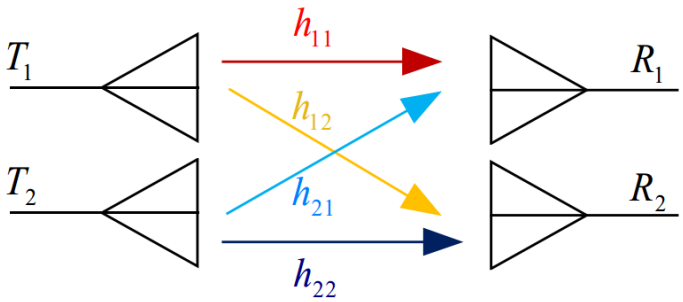

Figure 2.2: Representation of a MIMO channel.

[1] A new link corresponds to one additional transmitting-receiving antenna pair

In a MIMO scheme, the equivalent representation is given by

$$\mathbf{y} = \mathbf{H}\mathbf{x} + \mathbf{n}\,, \tag{2.3}$$

where **y** and **x** are column vectors with the signal at the receivers and transmitters, respectively, **n** is the channel noise vector, and **H** is a matrix with all the time domain channel responses, also called channel information[2]. Once again, if the channel information is known, only a matrix inversion is needed so as to estimate the transmitted signal from the received signal (assuming that **H** is a non-singular square matrix). Sadly, not only a real channel contains a combination of noise, phase shifts and time-delays, but also the transmitted signals' power decreases with the distance traveled [18]. Many mobile channels also include awful phenomena such as multipath propagation (which results in a time dispersion), selective frequency fading, scattering or Doppler shifts [17]. To cope with any of this undesired effects, the recovery of the transmitted signals becomes a complexity giant in a MIMO scenario, expanding with the number of transmitted signals.

2.1.2 MIMO Channel Capacity

Computational complexities aside, by using T MIMO links, the maximum spectral efficiency increases by up to a factor of T. However, this scheme would uses T times the power if the power per link is kept. Since most devices have power restrictions, the idea of using T links (with the same power per link) to get T times the maximum spectral efficiency is not much of a breakthrough. A more useful measure would be a comparison of the channel capacity with the extra links, while keeping the total transmitted power the same.

From [5] and [6], if both the receiver and the transmitter have access to the channel information, the MIMO capacity for a system with P transmitting antennas and N receiving antennas (therefore, T is the minimum between N and P) can be given as

$$C = B \max_{Tr(\mathbf{R}_{xx})=P} \log_2 \det\left(\mathbf{I}_N + \frac{SNR}{P}\mathbf{H}\mathbf{R}_{xx}\mathbf{H}^H\right), \tag{2.4}$$

where Tr denotes the trace operator, $\mathbf{R}_{xx}$ the autocorrelation matrix of the transmitted signal[3], det is the determinant of a square matrix, $\mathbf{I}_N$ is an identity matrix with size N and SNR is the global SNR of the system. The $\mathbf{R}_{xx}$ can also be seen as the power distribution among the transmitters and, as the transmitted signals are independent most of the times, it is a diagonal matrix.

[2] In this section, for the sake of a coherent explanation and to differentiate from the SISO channel, bold capital **H** is used to represent the time domain MIMO channel, instead of being the frequency domain representation of the channel response, as will be denoted in the following chapters.

[3] The autocorrelation matrix of a given vector **x** is given by $\mathbf{R}_{xx} = E\left\{\mathbf{x}\mathbf{x}^H\right\}$, with $E\{\}$ denoting the expectation operator

Typically, the total power is distributed by the transmitting antennas according to the channel conditions [17]. However, if the transmitter doesn't possess the channel information, it is assumed an equal power distribution among the transmitters, in which case $\mathbf{R}_{xx}$ is an identity matrix and equation (2.4) becomes

$$C = B\log_2 \det\left(\mathbf{I}_N + \frac{SNR}{P}\mathbf{H}\mathbf{H}^H\right). \tag{2.5}$$

Assuming that $\mathbf{H}\mathbf{H}^H$ is normalized (i.e. the square of the diagonal elements is 1), with further mathematical simplifications (as in [19] and [17]) equation (2.5) becomes

$$C = BT\log_2(1+SNR) + B\log_2 \det(\mathbf{R}_{ch}), \tag{2.6}$$

where $\mathbf{R}_{ch}$ is the normalized channel correlation matrix, such as its elements $|r_{i,j}| \leq 1$ and

$$r_{i,j} = \sum_k h_{i,k} h^*_{k,j}. \tag{2.7}$$

Knowing the maximum value that each element can take, it becomes clear that $\det(\mathbf{R}_{ch})$ is at most 1 and, therefore, channel correlation degrades the maximum spectral efficiency (as shown in Fig. (2.3)). At a first, light approach, the previous statement seems both obvious and contradictory. From one side, when the channels are correlated, then clearly we have less information to exploit and, therefore, an overall worse performance. From

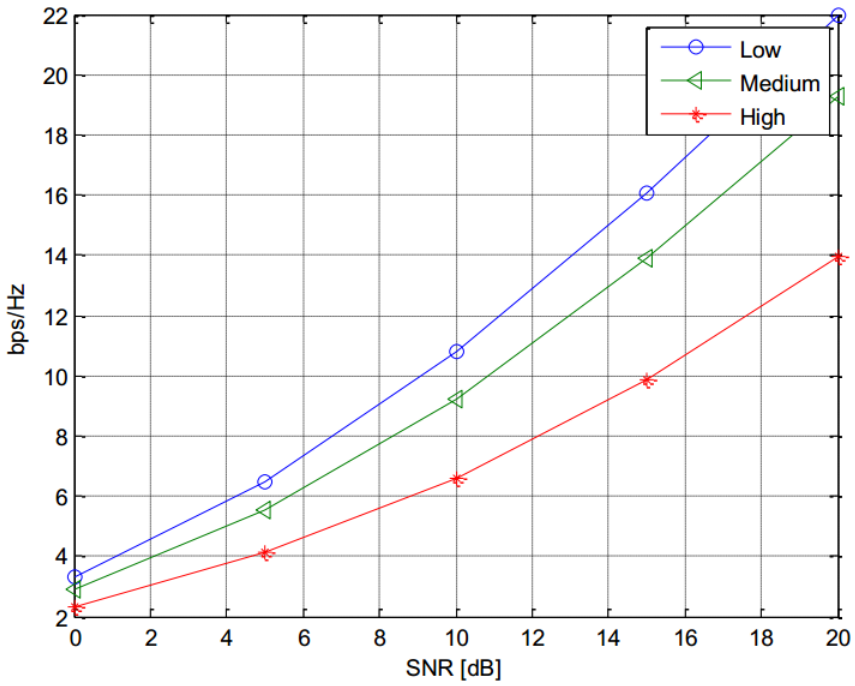

Figure 2.3: Maximum spectral efficiency *vs* SNR on a 4x4 MIMO, for three levels of correlation (low = 0%, medium = 20% and high = 40%) [17].

the other, an uncorrelated channel requires the presence of nefarious channel effects, such as multipath propagation (which results in a time dispersion), selective frequency fading, scattering or Doppler shifts [17]. Nonetheless, going back to the most basic concepts such as equation (2.3), it is evident that the channel matrix needs to have both its rows and columns uncorrelated, as the matrix inversion would be impossible otherwise. A MIMO scheme is then a somewhat elusive system: to bring out its utter potential, it needs to be under situations whose complexity was already very high for SISO systems [17].

If the channel information is uncorrelated, then the maximum spectral efficiency increases linearly with T, the minimum between the number of transmitting and receiving antennas, as shown in Fig. (2.4). Even though some assumptions were made before reaching to equation (2.6), the generalization proves that the same conclusions can be taken [17]. Disregarding the complexity at the receivers, employing MIMO systems is then a straightforward mean to greatly improve the spectral efficiency, while keeping the same power consumption at the transmitter [7] [2].

Just as a final remark: for MU-MIMO, the exact same conclusions can be made. However, it has several users in the same physical channel and it is generally undesired to lower the throughput per user (when compared to a SISO channel). Therefore, it is not as linear to compare the spectral efficiency gain when changing a given system from SISO

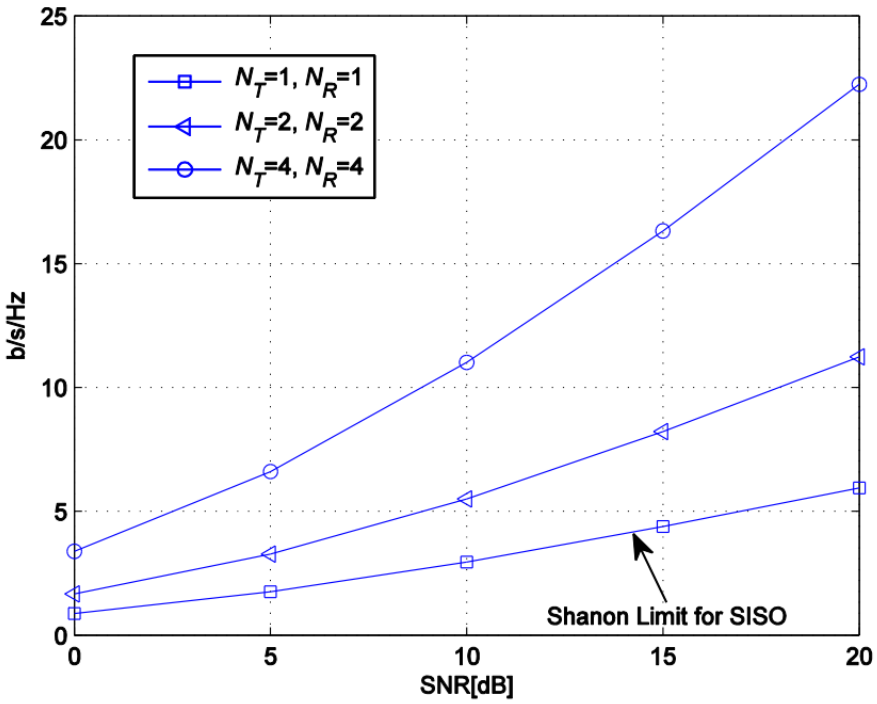

Figure 2.4: Maximum spectral efficiency *vs* SNR comparison for uncorrelated channels [17].

to MU-MIMO, as there will be both MIMO and total power gains.

2.2 Signal Separation for Uplink MIMO

By considering a MIMO system with a number of antennas at the receiver at least equal to the number employed at the transmitter (i.e. $P \leq N$), it is theoretically possible to separate the P different signals [10]. On flat frequency fading MIMO channels the signal separation is quite simple [10], needing only to invert the channel matrix (as described previously). However, for frequency-selective channels, signal separation requires the implementation of more complex inter-antenna interference cancellation schemes. For optimal performance of the interantenna interference cancellation scheme, signal separation and equalization should be performed together iteratively [10]. This is easily justified, considering that the for a given signal estimation it is needed an equalization and, to produce an improved estimation through inter-antenna interference cancellation, previous signals' estimations are needed. In that sense, a MIMO equalizer not only compensates the linear distortion causer by the channel frequency selectivity, but also performs signal separation.

The first MIMO equalizers proposed were time domain (TD) systems [20–22]. Unfortunately, as with other TD receivers, their complexity can be quite high for severely time-dispersive channels. On the other hand, for systems with frequency domain (FD) processing, the equalizer complexity can be kept low since most channels can be modeled as tiny parallel flat fading channels, being the recommended equalization scheme [8]. Amongst the FD equalization schemes for the uplink MIMO channel, the IB-DFE has shown the most promising results [10], being the subject of the following chapter.

3

MIMO IB-DFE Receivers

Contents

In order to be successful, any kind of mobile communications must be able to withstand inter-carrier and inter-symbol interference, caused by the possible strong dispersive nature of the channel. To be able to transmit over severe time-dispersive channels, the best option for uplink MIMO communications is to have an appropriate cyclic extension (CE) and to be combined alongside block-based frequency domain equalization (FDE) transmission techniques [23] [10]. For any uplink transmission, single carrier (SC) modulation schemes with FDE are proved to be the best suited [24], due to the lower peak-to-average power ratio (PAPR) [25] and to the possibility to replace the linear FDE with a non-linear FDE. Amongst the non-linear FDE, the IB-DFE scheme delivers the greatest gains in performance [8] [10], being the subject of this chapter.

3.1 SISO IB-DFE Receivers

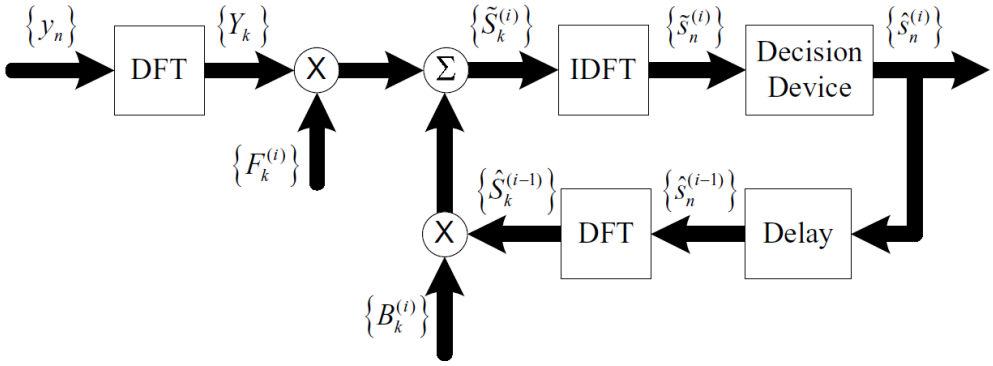

Figure 3.1: Block diagram representation of a SISO IB-DFE receiver [26].

Before the MIMO implementation of the IB-DFE algorithm, the IB-DFE existed as a SISO equalizer for block based SC transmissions [8] [10], with its main diagram being represented in Fig 3.1. For a SISO system, the IB-DFE equalizer is, as described on its own name, an iterative block decision feedback equalizer in the frequency domain. To a given received block signal, the SISO IB-DFE algorithm would compute two sets of coefficients, the feedback and the feedforward coefficients, as shown in Fig. 3.1. The feedforward coefficients aim to equalize the channel, with the knowledge of the channel information, while the feedback coefficients aim to both minimize the intersymbol interference (ISI) and the interference due to past incorrect estimations. Iteratively performing this algorithm would yield a better and better estimation of that given block. Considering this block isolation capability, a MIMO version of this algorithm was created.

3.2 Basic Structure of the MIMO IB-DFE Receivers

The MIMO IB-DFE receiver extends the basic SISO IB-DFE principle of residual interference's cancellation, based on known data estimations from feed-forward equalization. When attempting to recover the P different transmitted streams using the N receiving antennas, the relationship $P \leq N$ is required (as explained previously). Essentially, MIMO IB-DFE [9] detects one stream at a time and cancels the interference from already detected streams, a method also known as successive interference cancellation (SIC). To maximize this method's effectiveness, it is desirable to rank the streams according to some quality measure (usually the average received power) and to detect the streams from the best to the worst. That way, the interference of the stronger streams is diminished when attempting to detect the weaker ones, which proves to be extremely difficult otherwise. This algorithm aims then to perform frequency-domain equalization while minimizing the interference between streams, with both feedback and feedforward filters. The algorithm works on a per-block basis, meaning that the feedback's effectiveness to cancel all the interferences is limited by the reliability of the detected data at previous iterations. Consequently, it is desired to apply more than one iteration per block, in order to successfully detect all the streams. A general block diagram representation of the MIMO IB-DFE is shown in Fig. 3.2.

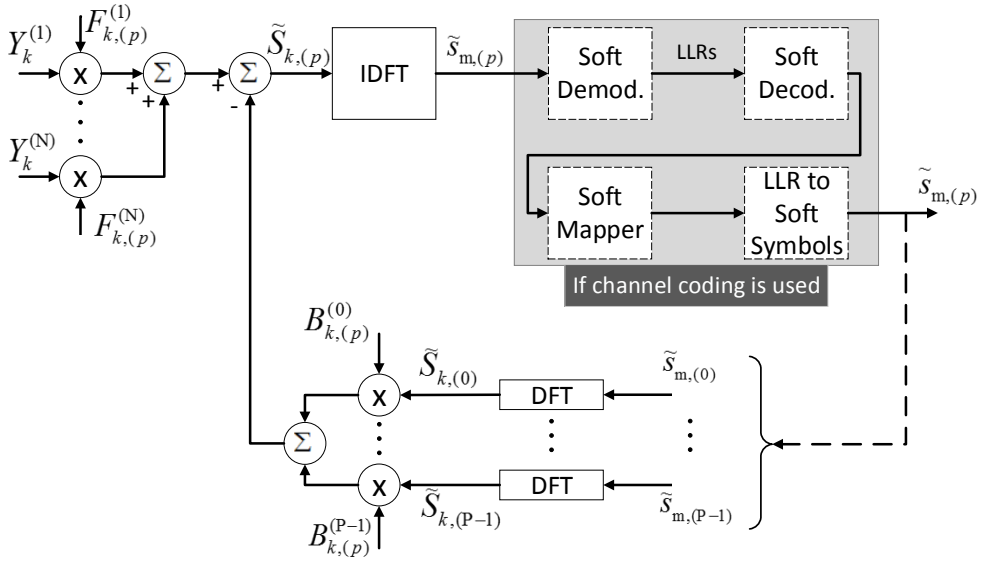

Figure 3.2: Detection of the pth layer, for a given iteration in MIMO IB-DFE.

Let the time-domain blocks of length M at the pth transmitting antenna and nth receiving antenna be respectively

$$\mathbf{s}_{(p)} = \left[s_{1,(p)} \cdots s_{M,(p)} \right]^T \tag{3.1}$$

and

$$\mathbf{y}^{(n)} = \left[y_1^{(n)} \cdots y_M^{(n)} \right]^T , \tag{3.2}$$

with $p = 1, \cdots, P$, and $n = 1, \cdots, N$ and let

$$\mathbf{S}_{(p)} = \left[S_{1,(p)} \cdots S_{M,(p)} \right]^T \tag{3.3}$$

and

$$\mathbf{Y}^{(n)} = \left[Y_1^{(n)} \cdots Y_M^{(n)} \right]^T \tag{3.4}$$

denote the M-point discrete Fourier transform (DFT) of $\mathbf{s}_{(p)}$ and $\mathbf{y}^{(n)}$, where

$$S_{k,(p)} = \sum_{m=0}^{M-1} s_{m,(p)} e^{(-j2\pi km/M)} \tag{3.5}$$

and

$$Y_k^{(n)} = \sum_{m=0}^{M-1} y_m^{(n)} e^{(-j2\pi km/M)} , \tag{3.6}$$

With $\mathbf{S}_k$ and $\mathbf{Y}_k$ being respectively the P-tuple and N-tuple vectors of the obtained DFT coefficients for each k sub-carrier, with $k = 0, \cdots, M-1$, given by

$$\mathbf{S}_k = \left[S_{k,(1)} \cdots S_{k,(P)} \right]^T \tag{3.7}$$

and

$$\mathbf{Y}_k = \left[Y_k^{(1)} \cdots Y_k^{(N)} \right]^T , \tag{3.8}$$

the receiving frequency-domain signal $\mathbf{Y}_k$ can be written as

$$\mathbf{Y}_k = \mathbf{H}_k \mathbf{S}_k + \mathbf{N}_k , \tag{3.9}$$

where, $\mathbf{H}_k$ and $\mathbf{N}_k$ represent respectively the frequency-domain dispersive channel and additive white gaussian noise (AWGN) matrices, written as

$$\mathbf{H}_k = \begin{bmatrix} H_{k,(1)}^{(1)} & \cdots & H_{k,(P)}^{(1)} \\ \vdots & \ddots & \vdots \\ H_{k,(1)}^{(N)} & \cdots & H_{k,(P)}^{(N)} \end{bmatrix} \tag{3.10}$$

where $H_{k,(p)}^{(n)}$ is the channel's frequency response for the k-th carrier between the p-th transmitter and the n-th receiver, and

$$\mathbf{N}_k = \left[N_k^{(1)} \cdots N_k^{(N)} \right]^T . \tag{3.11}$$

The frequency-domain soft-estimations associated with the pth layer at the output of the equalizer are given by

$$\widetilde{\mathbf{S}}_k = \mathbf{F}_k^T \mathbf{Y}_k - \mathbf{B}_k^T \widetilde{\mathbf{S}'}_k , \tag{3.12}$$

where the feedforward and feedback matrices are respectively

$$\mathbf{F}_k = \begin{bmatrix} F_{k,(1)}^{(1)} & \cdots & F_{k,(P)}^{(1)} \\ \vdots & \ddots & \vdots \\ F_{k,(1)}^{(N)} & \cdots & F_{k,(P)}^{(N)} \end{bmatrix} \tag{3.13}$$

and

$$\mathbf{B}_k = \begin{bmatrix} B_{k,(1)}^{(1)} & \cdots & B_{k,(P)}^{(1)} \\ \vdots & \ddots & \vdots \\ B_{k,(1)}^{(P)} & \cdots & B_{k,(P)}^{(P)} \end{bmatrix} . \tag{3.14}$$

$F_{k,(p)}^{(n)}$ and $B_{k,(p)}^{(p)}$ denote the feedforward and feedback filters coefficients and the vector $\widetilde{\mathbf{S}}'_k$ contains the DFT of the time-domain blocks associated with latest estimations for the transmitted symbols (for the first iteration those terms are zero).

3.2.1 Hard IB-DFE Reliability

The frequency-domain samples used in the feedback loop can produce hard-estimations, $\widehat{\mathbf{S}}_k$, by taking hard decisions on $\widetilde{\mathbf{S}}_k$, which can be further written as

$$\widehat{\mathbf{S}}_k = \mathbf{P}\mathbf{S}_k + \Delta_k \ , \tag{3.15}$$

with the length-P column vector

$$\Delta_k = \left[\Delta_{k,(1)} \dots \Delta_{k,(P)}\right]^T , \tag{3.16}$$

denoting the frequency domain noise plus interference (for the hard-estimation) and

$$\mathbf{P} = \mathrm{diag}(\rho_{(1)}, \dots, \rho_{(P)}) \tag{3.17}$$

being a diagonal matrix with the reliability of the detected hard symbols, measured by the correlation coefficients in (3.17). Those correlation coefficients are given by

$$\rho_{(p)} = E[S_{k,(p)} S_{k,(p)}^*]/E[|S_{k,(p)}|^2] = E[\widehat{s}_{m,(p)} s_{m,(p)}^*]/E_S \ , \tag{3.18}$$

where

$$E_S = E[|s_{m,(p)}|^2] = E[|S_{k,(p)}|^2]/M \tag{3.19}$$

is the average symbol energy, common to all layers. Since $E[\Delta_{k,(p)} S_{k',(p)}^*] \approx 0$, the power of the total noise plus interference can given by

$$E[|\Delta_{k,(p)}|^2] \approx (1-\rho_{(p)}^2) M E_S \ . \tag{3.20}$$

3.2.2 Soft IB-DFE Reliability

The correlation coefficient can be estimated from the time-domain samples associated with the equalizer output, $\widetilde{s}_{m,(p)}$, as described in [27].

It can also be shown that time-domain samples associated with the equalizer output, $\widetilde{\mathbf{s}}_m$, can be written as

$$\widetilde{\mathbf{s}}_m = \Gamma \mathbf{s}_m + \mathbf{E}_m^{eq} \ , \tag{3.21}$$

where $\mathbf{s}_m$ and $\widetilde{\mathbf{s}}_m$ denote the P size vectors with the time-domain signals and the time-domain equalizer's soft outputs, respectively. The E_m^{eq} and Γ matrices are given by

$$\mathbf{E}_m^{eq} = \left[\varepsilon_{m,(1)}^{eq} \cdots \ \varepsilon_{m,(P)}^{eq}\right]^T , \tag{3.22}$$

where $\varepsilon_{m,(p)}^{eq}$ denotes the overall noise plus interference on the detected stream p, and

$$\Gamma = \mathrm{diag}(\gamma) \tag{3.23}$$

is a sized P column vector containing the reliability of estimated soft symbols, given by[1]

$$\gamma = \frac{1}{M} \sum_{k=0}^{M-1} [\mathbf{1}_{1\times N}(\mathbf{H}_k \odot \mathbf{F}_k)]^T \ . \tag{3.24}$$

The corresponding frequency-domain samples can be written as

$$\widetilde{\mathbf{S}}_k = \Gamma \mathbf{S}_k + \mathbf{E}_k^{Eq} \ , \tag{3.25}$$

where the $\varepsilon_{k,(p)}^{Eq}$ $(k = 0, \cdots, M-1)$ terms of the P-sized vector E_k^{Eq} are the DFT of $\varepsilon_{m,(p)}^{eq}$ $(m = 0, \cdots, M-1)$. The signal to interference plus noise ratio (SNIR) of the p-th transmitter for the k-th carrier measured in the frequency domain is written as

$$SNIR_{k,(p)}^{F} = \frac{|\gamma_{(p)}|^2 M E_S}{\left[|\varepsilon_{k,(p)}^{Eq}|^2\right]} \ . \tag{3.26}$$

3.2.3 Deriving the IB-DFE coefficients

After combining equations (3.12) and (3.26) and using Lagrange multipliers so as to maximize equation (3.26) [26], the optimum feedback coefficients at a specific iteration are

$$\mathbf{B}_k = \mathbf{P}(\mathbf{F}_k^T \mathbf{H}_k - \Gamma) \ . \tag{3.27}$$

The feedforward coefficients, required by (3.27) and (3.24), are obtained from the following equation:

[1] $\odot$ represents the pointwise matrix multiplication

$$\mathbf{F}_k = (\mathbf{I}-\mathbf{P}^2)\Gamma\mathbf{H}_k^H \left[(\mathbf{I}-\mathbf{P}^2)\mathbf{H}_k^H\mathbf{H}_k + \frac{P}{SNR_{(p)}}\mathbf{I}\right]^{-1} , \tag{3.28}$$

where the SNR at each receiving antenna is

$$SNR_{(p)} = (PE_S)/(2\sigma_N^2) , \tag{3.29}$$

being σ_N^2 the variance of the real and imaginary parts of the channel noise. Clearly, the feedforward and feedback coefficients take into account both hard and soft reliabilities of each detected block. In the next section we will explore this feature, using it to further improve the system.

3.2.4 Coding and Turbo IB-DFE

Transmission systems rely on channel coding for recovering from transmission errors. Decoding can be carried on after equalization, but better results are obtained by bringing it into the IB-DFE loop. When a IB-DFE scheme is merged with coding/decoding, it is also called turbo equalization in the frequency domain [10]. Since the data that is fed between IB-DFE iterations is the soft estimation of the current block symbols, we can use channel coding to obtain an improved soft estimation and to feed back that estimation instead. This turbo equalization, represented in Fig. 3.2, not only improves overall performance, but also allows for higher levels of interference to be acceptable in our proposed application. Please notice that if the dotted blocks were removed, Fig. 3.2 would be a representation of a non-turbo IB-DFE.

For the specific case of quadrature phase-shift keying (QPSK) symbols with points $\{\pm 1 \pm j\}$, soft demapping and mapping is greatly simplified, becoming very easy to deploy. Defining the complex log likelihood ratio for the p-th transmitted block's m-th time domain symbol as

$$\lambda_{m,(p)} = \lambda_{R,m,(p)} + j\lambda_{I,m,(p)} , \tag{3.30}$$

where $\lambda_{R,m,(p)}$ and $\lambda_{I,m,(p)}$ are associated (respectively) to $\mathrm{Re}[s_{m,(p)}]$ and $\mathrm{Im}[s_{m,(p)}]$, the soft demapper yields [28]

$$\lambda_{m,(p)} = \frac{4\widetilde{s}_{m,(p)}}{\sigma^2_{SD,(p)}} , \tag{3.31}$$

with $\sigma^2_{SD,(p)}$ being the variance of the complex noise after the equalization. This means that the log likelihood ratio is proportional to the equalizer soft output. In turn, if $\eta_{m,(p)} = \eta_{R,m,(p)} + j\eta_{I,m,(p)}$ is the complex log likelihood ratio at the decoder output (extrinsic information), we can further improve the equalizer soft output by making

$$\widetilde{s}_{m,(p))} = \tanh\left(\frac{\eta_{R,m,(p)}}{2}\right) + j\tanh\left(\frac{\eta_{I,m,(p)}}{2}\right) . \tag{3.32}$$

After understanding the different MIMO IB-DFE configurations, the reader is ready to fully grasp the changes proposed on this thesis, starting in the following chapter.

4

Improved Power and Spectral Efficiencies on MIMO Systems

Contents

After analyzing the potential of a MIMO channel and studying the IB-DFE scheme, this chapter focuses on improving both the power and the spectral efficiency of MIMO IB-DFE systems. To do so, section 4.1 targets the mobile user's power efficiency, while sections 4.2 and 4.3 are centered around spectral efficiency improvements.

4.1 MIMO SC Transmission using Magnitude Modulation Techniques

PAPR and spectral efficiency are two key elements when projecting a communications system. The first element is becoming a major issue for uplink communications, as to comply with the greater bandwidth limitations the transmitter must employ lower roll-off RRC filters and higher constellation orders, leading to a greater PAPR. A high PAPR not only requires demanding specifications from both the digital-to-analog converter (DAC) and the high power amplifier (HPA) used by the transmitter, increasing the price of those components, but also leads to smaller power efficiency. This inferior power efficiency, a major constraint for mobile users, is due to the increased HPA's back-off, an unpleasant but needed change if a distortionless transmission is desired.

A great way to improve the efficiency of SC based systems is to perform polyphase magnitude modulation [29, 30] of the signal to transmit. By trying to suppress peaks from the transmitted signals, we are able to reduce the PAPR, which reduces the HPA's back-off. Results have shown that between BER performance losses and power efficiency gains from the reduced HPA's back-off, we have a high net power gain, even for severe time-dispersive scenarios [31]. MM creates then the possibility to transmit more power while delivering the same maximum power to the HPA with very little computational effort, being a major asset for MIMO systems. It was also shown that these results can be improved using channel coding, which reduces the BER performance losses [29, 32].

4.1.1 Magnitude Modulation

Figure 4.1 introduces a typical SC transmitter, with the basic building blocks to allow for a successful communication. When the transmitted symbols are mapped in constant-envelope constellations, the main contribution for high PAPR on the transmitted signal comes from the pulse-shaping filter (normally RRC). Taking this into account, a symbol readjustment procedure could be employed prior to filtering to reduce the signal's envelope excursion. This is the basic concept of the MM method, similar to the adaptive peak-suppression algorithm for M-PSK type constellations proposed by Miller *et al.* [33].

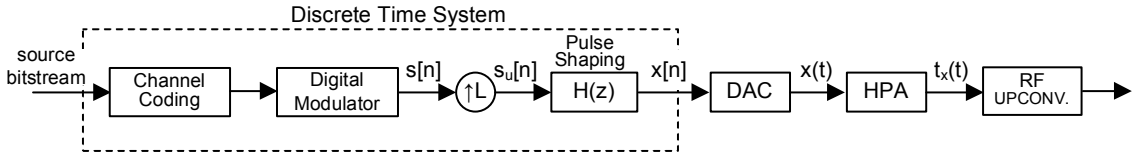

Figure 4.1: Generic SC transmitter scheme [34].

Figure 4.2 illustrates the MM principle [35] [33] [36]. Despite the different ways to apply this method, each MM implementation is composed of the following steps:

- predicting the response of the pulse shaping filter to a given symbol sequence of $s[n]$ (depending on the filter length),
- detect the peaks of the predicted response and calculate the corresponding scaling factor,
- multiplying the symbol s_n[1] for its MM coefficient m_n.

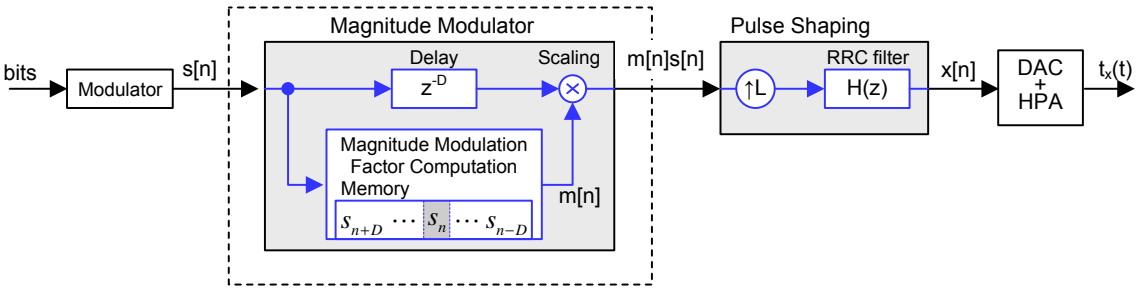

Figure 4.2: Magnitude modulation principle [34].

In order to correctly calculate each symbol's MM coefficient it is necessary to consider the RRC filter's length, to account for all the symbols that significantly contribute to the signal's amplitude (seen in figure 4.2 as the D past and future neighbors of the highlighted symbol). Therefore, this operation inserts a small time delay DT_{symb}, where T_{symb} is the symbol's duration.

In the peak detection step, there are two possible criteria to enforce: polar clipping (PC) and rectangular clipping (RC). When polar clipping is employed, the MM coefficient to be applied to s_n considers the amplitude of the predicted response sequence and compares it to a given threshold A, whereas a rectangular clipping type of approach evaluates the in-phase and quadrature components separately, with threshold levels A_I and A_Q.

[1] s_n refers to the particular sample at instant n, where $s[n]$ regards the discrete time sequence. The same notation is applied to the MM coefficients.

The scaling operation follows a similar reasoning. A rectangular scaling (RS) approach scales the in-phase and quadrature symbol components separately (i.e. each symbol needs two MM coefficients, one for each symbol component), as follows:

$$x[n] = \left[\sum_k m^I[k]\, s^I[k]\, \delta[n-kL]\right] * h[n] \; + \left[\sum_k m^Q[k]\, s^Q[k]\, \delta[n-kL]\right] * h[n] \; . \tag{4.1}$$

On the other hand, a method using polar scaling (PS) multiplies each symbol s_n with one coefficient m_n:

$$x[n] = \left[\sum_k m[k]\, s[k]\, \delta[n-kL]\right] * h[n] \; . \tag{4.2}$$

Despite adding some phase modulation, an RS approach provides a finer control of the envelope excursions over the other method, since it has an additional degree of freedom.

The existing MM techniques consist in the look-up table (LUT) method [36] [35], where the MM coefficients are pre-calculated and stored in a table, and the multistage polyphase magnitude modulation (MPMM) method [34], where the coefficients are calculated in real time. The MPMM procedure is fairly simple and it is scalable for constellations with $M \geq 16$ symbols, with net back-off gain[2] over 4dB [29] [34], surpassing the LUT method as the MM state of the art procedure.

4.1.2 MIMO with IB-DFE and MM

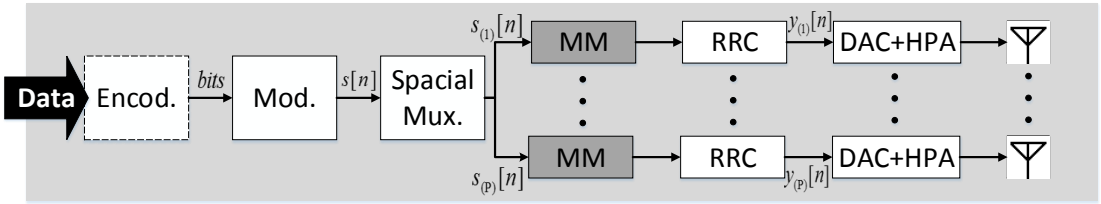

Figure 4.3: General diagram of the proposed transmitter.

One way of improving the power efficiency of a MIMO system is to control the envelope of the signal after the pulse shaping filter. A straightforward solution is to apply MM to each transmitting antenna. Thus, in this section it is proposed a MIMO system with a transmitter as specified in Fig. 4.3 and a IB-DFE receiver. The symbols to be transmitted are multiplexed into P parallel data streams $s_{(p)}[n]$ with $p = 1, \cdots, P$. Each

[2]This measurement accounts for the back-off gain in the transmitter and the distortion losses at the receiver for a given BER level.

stream is magnitude modulated in order to limit the excursion of the pulse shaped signal $y_{(p)}[n]$ feed to the DAC + HPA of antenna p, with $y_{(p)}[n]$ being given by,

$$y_{(p)}[n] = \sum_k m_{(p)}[k] s_{(p)}[k] h_{\mathrm{RRC}}[n-k] \ , \tag{4.3}$$

where $h_{RRC}[n]$ is the impulse response of pulse shaping filter (typically a RRC) and $m_{(p)}[n]$ is the MM factor applied to each symbol $s_{(p)}[n]$.

To compute $m_{(p)}[n]$ the MPMM algorithm is used, where it is guaranteed that

$$|y_{(p)}[n]|^2 \leq P_{(p),Max} \ , \tag{4.4}$$

with $P_{(p),Max}$ denoting the maximum admissible power at DAC + HPA of stream p. The magnitude modulated symbols are then transmitted through the P antennas, over a time dispersive channel. At the receiver, the MIMO IB-DFE scheme is used. As mentioned in [29], MM has better results when channel coding is used. The changes introduced in the time-domain symbols are quite small and a decoder can easily correct most errors, making the turbo IB-DFE [10] improvement a major asset for the proposed system.

4.1.3 Simulations Results

In the following simulations, all blocks are transmitted with the same amount of average power and when MM is used, only 1 MPMM stage is applied, considering the use of a 0.2 roll-off RRC filter. In order to compare BER *vs* SNR performance of different data streams at different iterations, we considered $P = 4$ data streams and a receiver with $N = 4$ antennas. The data streams' indexes indicate the order they are detected.

Simulations were performed over a channel model of [37], which has uncorrelated Rayleigh fading at all frequencies, as similar behaviors were observed for severe time-dispersive channels with rich multipath propagation (a typical urban scenario). At both the transmitter and the receiver side it was used a root-raised cosine (RRC) filter, to provide matched filtering and minimum intersymbol interference (ISI) (since its combined response is a raised cosine filter). For the sake of simplicity, it is assumed that the proposed schemes are under perfect synchronization and channel estimation conditions. Furthermore, the symbols were mapped using a QPSK modulation scheme, for implementation complexity issues.

In Figs. 4.4 and 4.5, we simulate the proposed system for a transmission not making use of channel coding, with and without MM. For this configuration, considering the same BER (at 10^{-4}), MM requires up to 2dB of extra SNR. From [29], the back-off reduction is about 4.4dB and thus we conclude that the system has a net gain of 2.2dB.

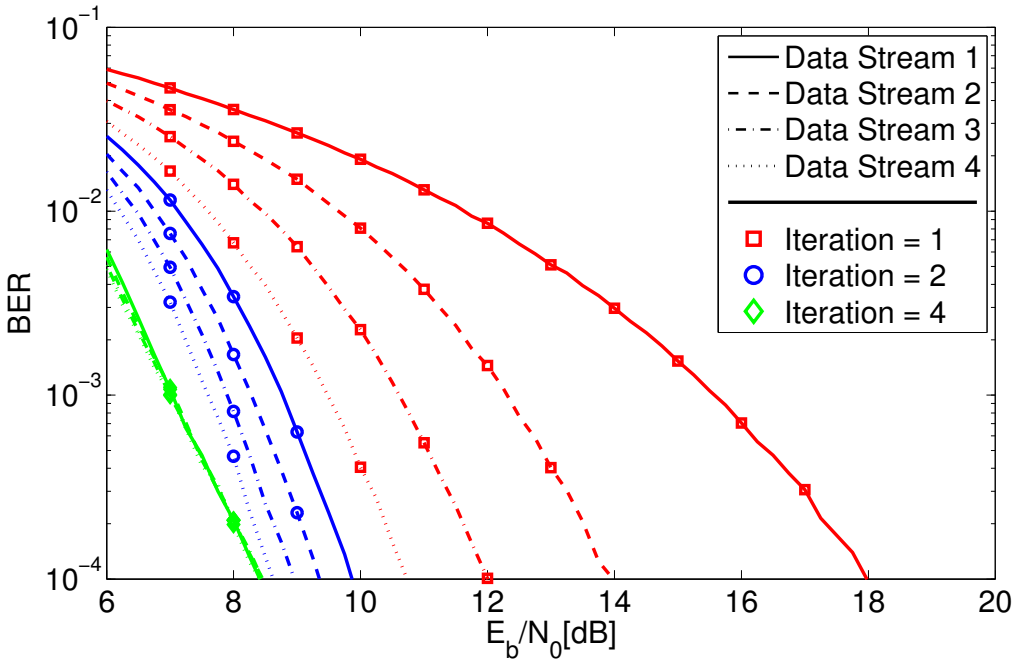

Figure 4.4: *BER vs* E_b/N_0 performance of the uncoded IB-DFE with no MM, for different layers at different iterations.

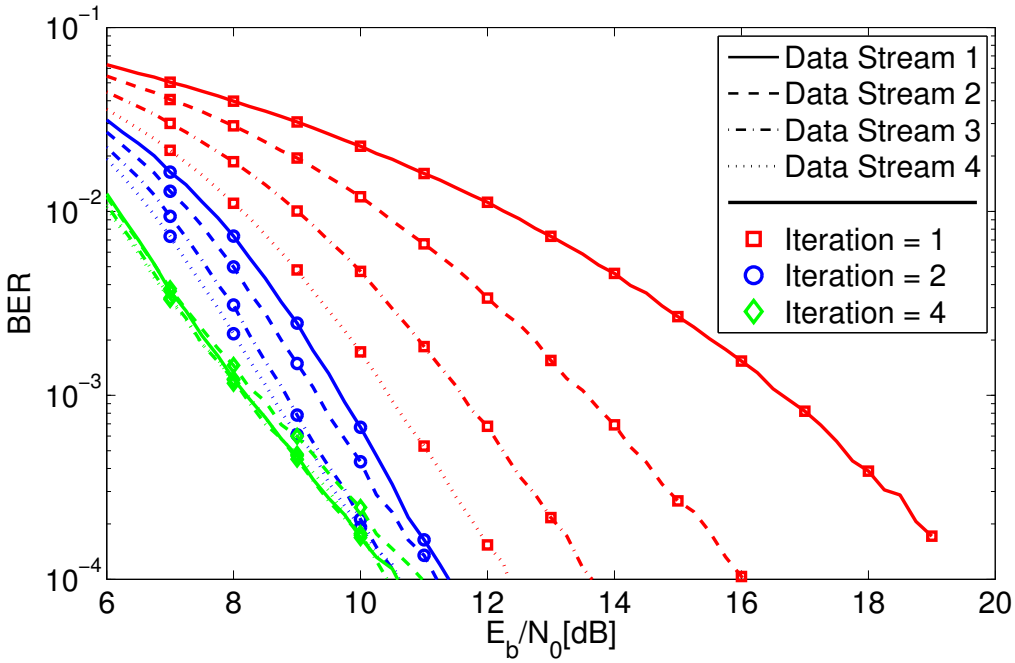

Figure 4.5: *BER vs* E_b/N_0 performance of the uncoded IB-DFE with MM, for different layers at different iterations.

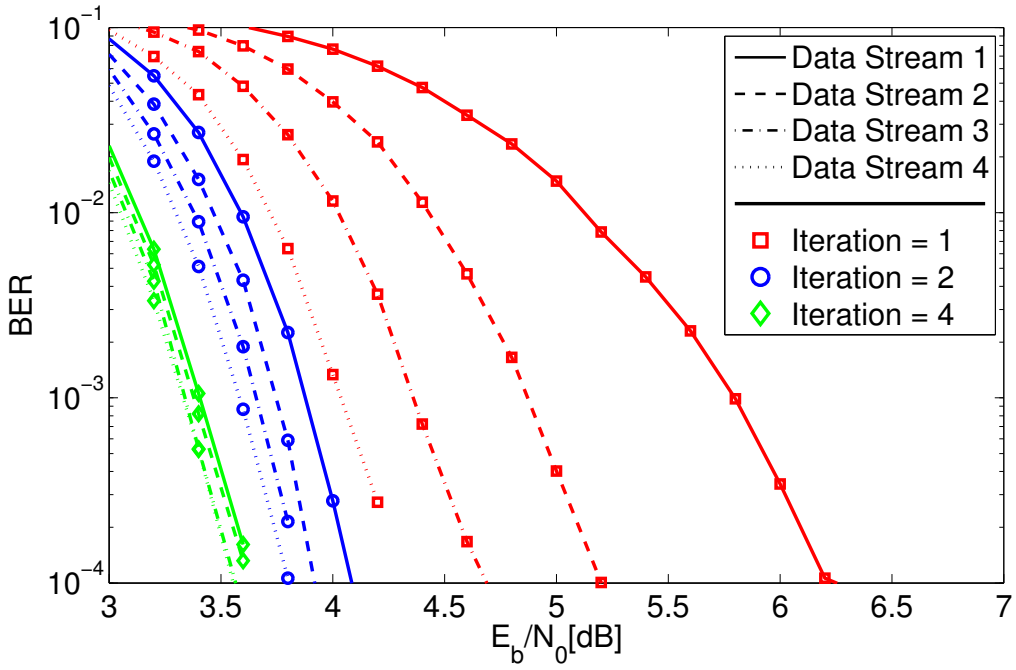

Figure 4.6: *BER vs* E_b/N_0 performance of the IB-DFE with turbo equalization and no MM, for different layers at different iterations.

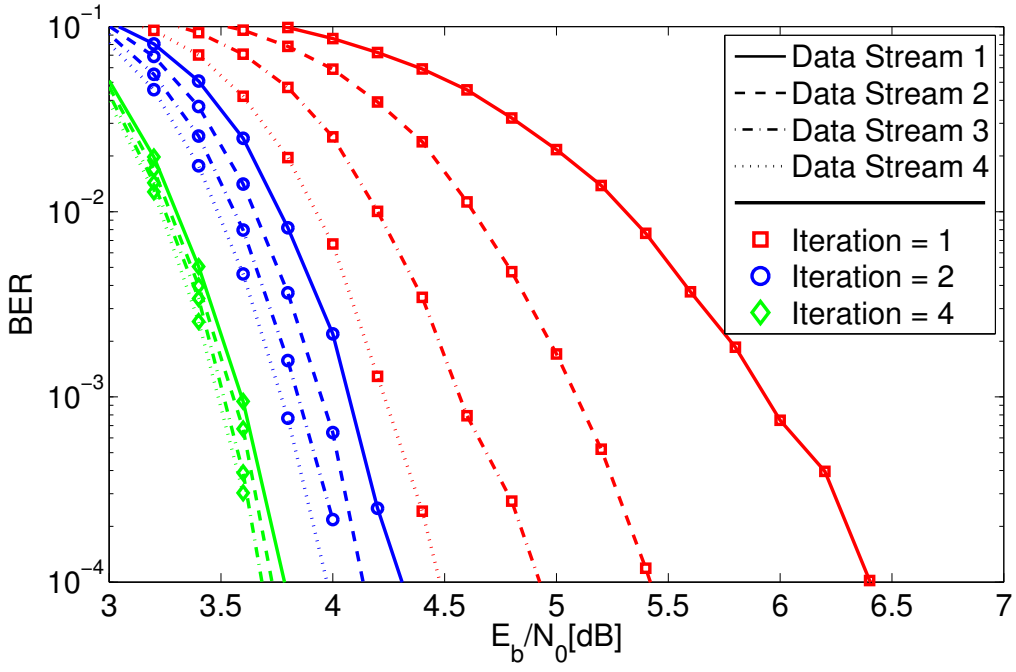

Figure 4.7: *BER vs* E_b/N_0 performance of the IB-DFE with turbo equalization and MM, for different layers at different iterations.

Applying a (1536,768) LDPC code and reworking the IB-DFE algorithm towards turbo equalization greatly improved our system, as shown in figures 4.6 and 4.7. Once

again, it's a comparison of the same system with and without MM. For this experiment and considering the same BER (at 10^{-4}), the MM only requires about 0.25dB of extra SNR, which combined with the 4.4dB gained from the HPA's back-off yields an outstanding net gain of 4.1dB.

4.1.4 Final Comments

A computational-wise effortless signal processing method (MM) was applied on a MIMO system, a system with quite a high complexity. MM can be easily applied to any currently working transmitter without any change in the receiver, providing a significant enhancement in power efficiency without interfering with the system's main function. The results obtained showed that if the system already uses coding, which always happens in modern communications, the net gain is truly remarkable.

4.2 Improved Spectral Efficiency with Cooperation

In conventional cellular architectures, different cells are considered independent of each other. Each cell is composed by a base station (BS), which handles several mobile terminals (MTs) that are exclusively bound to that BS until transferred to another one, in a process called handoff. As cells are treated as individual entities, it is needed to assign different frequency bands to neighbor cells, in order to avoid high irreversible interference levels. This frequency reuse factor leads to an overall spectral efficiency reduction, wasting precious transmission potential. Thus, if the frequency reuse factor applied could be reduced, it would be possible to increase the spectral efficiency and capacity of the overall wireless network [38] [11], up to the optimal scenario where every cell uses the same complete frequency band (i.e., a frequency reuse factor of one). To be able to reach this optimal case, the system must employ efficient interference management and/or interference cancellation techniques. This is specially true for users at the cell edge, as they have simultaneously a weak signal power at/from their designated BS and a high level of interference at/from other BSs. To oppose the aforementioned problems, cooperative multi-point techniques such as BS cooperation architectures can be employed. The basic idea behind BS cooperation is to assign the same physical channel for different MTs and to perform the detection in a centralized form, without requiring any extra effort from the MTs. Considering those characteristics, for uplink transmission a BS cooperation scheme can be compared to a MU-MIMO. The proposed scenario is presented in Fig. 4.8.

4.2.1 Base Station Cooperation combined with IB-DFE

Assume block-based SC transmission on the uplink communication. The data blocks are transmitted by P different MTs on partially overlapping cells, each cell associated to a given BS, over the same time-dispersive physical channel (i.e. they transmit simultaneously at the same frequency band). If the BSs of N partially overlapped cells are connected to a central unit through a high speed data link, as shown in figure 4.8, it is possible to perform real-time joint signal processing (i.e. IB-DFE) regarding those P users ($P \leq N$), improving the overall system performance.

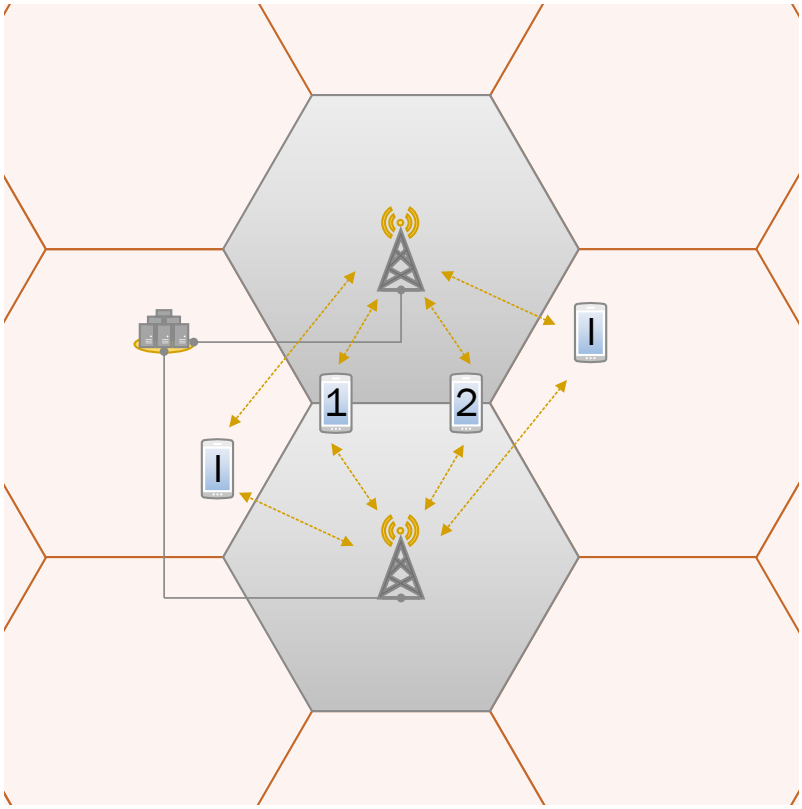

Figure 4.8: System representation, with $P = N = 2$. The MTs with 1 and 2 are the considered users, the ones with I are considered interference generators. It is considered that all MTs are using the same physical channel.

If a frequency reuse factor of 1 is considered (i.e., all the BSs use the same frequency band), it is likely that adjacent BSs have associated MTs that will use the same physical channel as our P considered MTs. Those additional MTs will be seen as added noise at the R considered BSs. As all the noise sources are independent, the total noise will be then

$$N_{k,total}^{(n)} = N_k^{(n)} + \sum_{u=1}^{U} H_{k,(P+u)}^{(n)} S_{k,(P+u)} \ , \tag{4.5}$$

with $n = 1, \cdots, N$ and where U is the total number of interfering MTs. Equation (3.9) should then be corrected to

$$\mathbf{Y}_k = \mathbf{H}_k \mathbf{S}_k + \mathbf{N}_{k,total} \ , \tag{4.6}$$

where

$$\mathbf{N}_{k,total} = \left[N_{k,total}^{(1)} \cdots N_{k,total}^{(N)} \right]^T . \tag{4.7}$$

Considering both channel and interfering users' noise at the cooperating BSs, it is possible to evaluate the magnitude of the performance gain for a given system configuration. Certainly, it is expected to exist a maximum level of interference beyond which the IB-DFE is unable to correctly distinguish the signals transmitted, rendering the possible performance gain useless. To counter this undesired limitation, channel coding [39] and a turbo equalization configuration [10] can be used, improving the receiver's performance and, therefore, reducing the interference effect [10]. This allows for higher levels of interference to be acceptable.

4.2.2 Simulations Results

In order to compare different power per user and interference levels, we considered $P = 2$ users and $N = 2$ receiving BSs and antennas (i.e., 1 antenna per BS). All data blocks are transmitted with the same amount of average power and, unless stated otherwise, the results after the 4th IB-DFE iteration are considered. All the considerations made in the subsection 4.1.3 relating to the system configuration (e.g. modulation, channel type, channel coding, etc) are also applicable here.

A useful (and therefore used) metric for performance comparison is the total interference, when compared to the desired signal's power. The total relative interference is given by the quotient between the total power of the interfering signals and the total power of the desired signals, as stated in equation (4.8). Please note that this total relative interference does not include the channel noise and, therefore, can be seen as the signal to interference ratio.

$$Total\ Interference = \frac{\sum_{u=1}^{U} H_{k,(P+u)}^{(n)} S_{k,(P+u)}}{\sum_{p=1}^{P} H_{k,(p)}^{(n)} S_{k,(p)}} \tag{4.8}$$

In Fig. 4.9, the aforementioned scheme is simulated for a group of average powers per user, in E_b/N_0, for various levels of total relative interference. As it can be observed, in order to obtain a good BER level for the 4th IB-DFE iteration (let's consider it 10^{-4}), it is needed both a decent level of power per user and the absence of high-power interference. The first ensures that the user's signal is powerful enough to persist over the channel

noise even in the absence of interference and, for the considered configuration, needs to be at least around 6dB[3] (measured in E_b/N_0). The second condition makes sure that the total noise seen by the MTs' signals is below the acceptable threshold for the IB-DFE algorithm. In an extreme scenario with a very high level of interference, the total noise is mostly interference. Given the previous definition of total interference in dB, it is observed that for the same BER performance, the total relative interference should be below -6 dB.

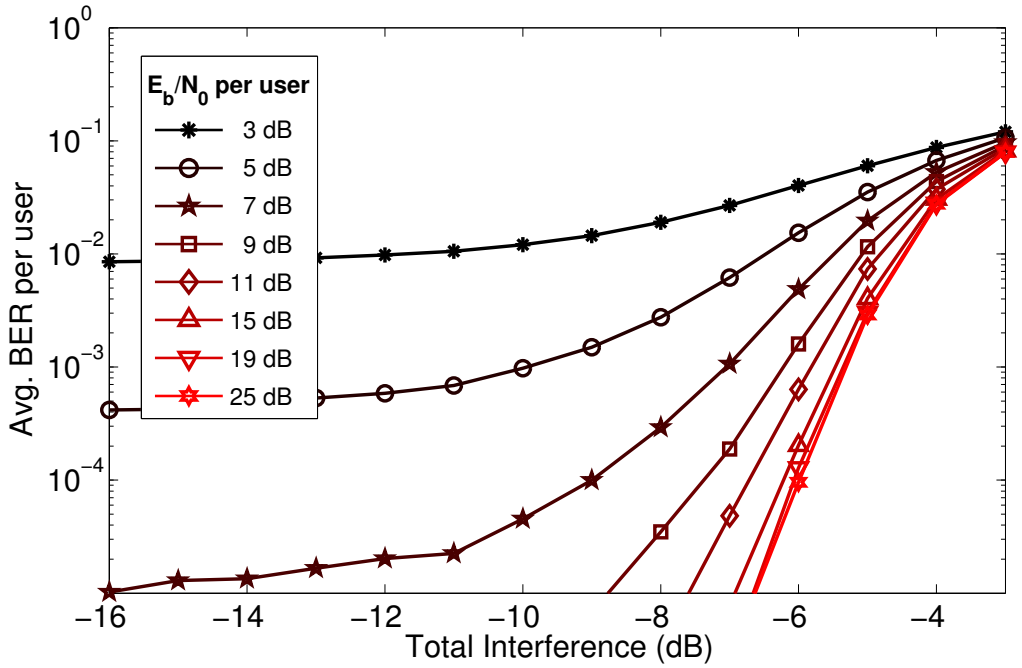

Figure 4.9: Average BER per user *vs* total interference for the 4th iteration of IB-DFE, considering various values for the power per user.

To compare the weight of the number of IB-DFE iterations Fig. 4.10 should be observed. Here it is plotted the average BER versus the average power per user, given a specific interference level. The performance increase per IB-DFE iteration decreases greatly with the number of iterations and, after the 4th iteration, the gain is almost negligible. From this simulation, it is also concluded that the performance increase per IB-DFE iteration increases as the relative interference level decreases and the power per user increases.

[3]This would correspond to the line between 5dB and 7dB in Fig. 4.9

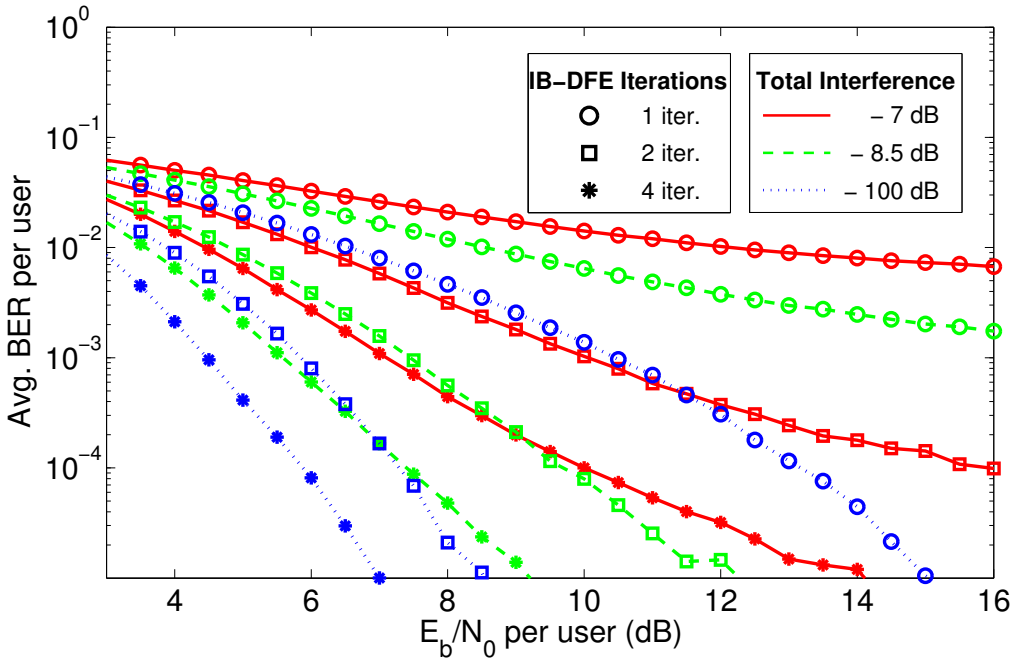

Figure 4.10: Average BER per user *vs* power per user for different iterations of IB-DFE, considering various interference levels.

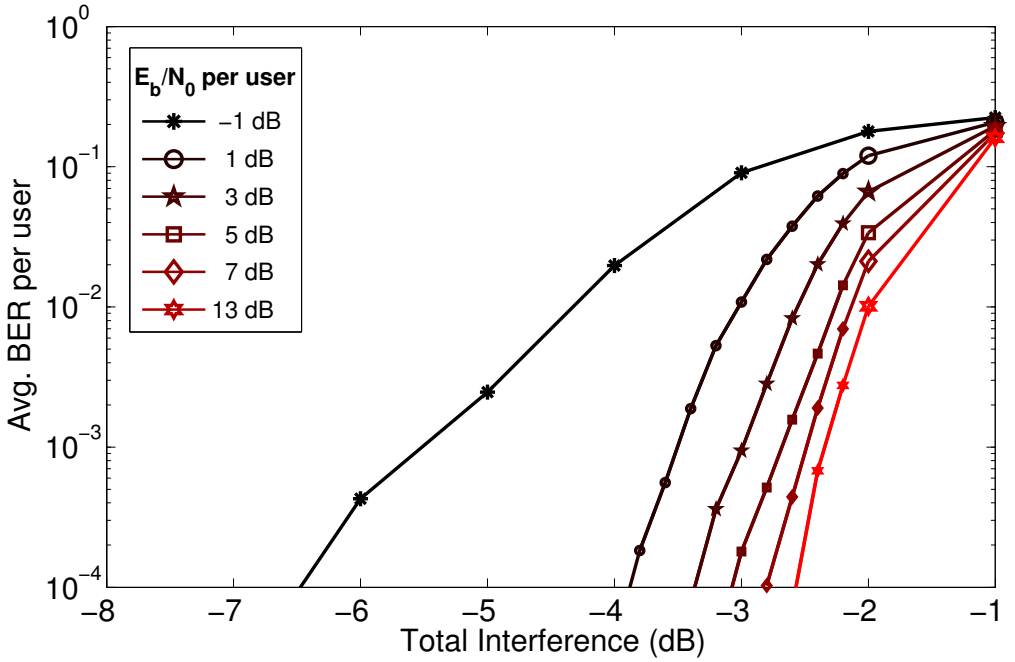

Figure 4.11: Average BER per user *vs* total interference for the 4th iteration of IB-DFE with LDPC coding (rate = 0.5) and turbo equalization, considering various values for the power per user.

Fig. 4.11 is obtained by applying LDPC coding with a code rate of $1/2$ and a turbo IB-DFE to a scenario similar to the first set of results of this subsection. As discussed in

the previous chapter, the turbo equalization scheme has a greatly improved performance, at the expense of some extra computational effort. For the same BER of 10^{-4}, the total relative interference can now be as high as -2.5dB, if the power per user is high enough. In other words, this means that our proposed scheme with LDPC coding and turbo equalization can withstand an interference with power as high as half of the considered MTs' transmitted power, while keeping a good BER performance.

Finally, a comparison between the same scheme with and without BS cooperation is made in Fig. 4.12. The system without BS cooperation used has only 1 MT and 1 BS (with 1 antenna), keeping the one MT to one antenna per physical channel ratio. For the same amount of absolute interference, the system with the BS cooperation outperforms the one without by a large margin. If a frequency reuse factor of 1 is chosen, not only the system with BS cooperation is better but also situations with 2 MTs sharing the same cell edges and the same physical channel (as in Fig. 4.8) would be infeasible, due to the high level of interference.

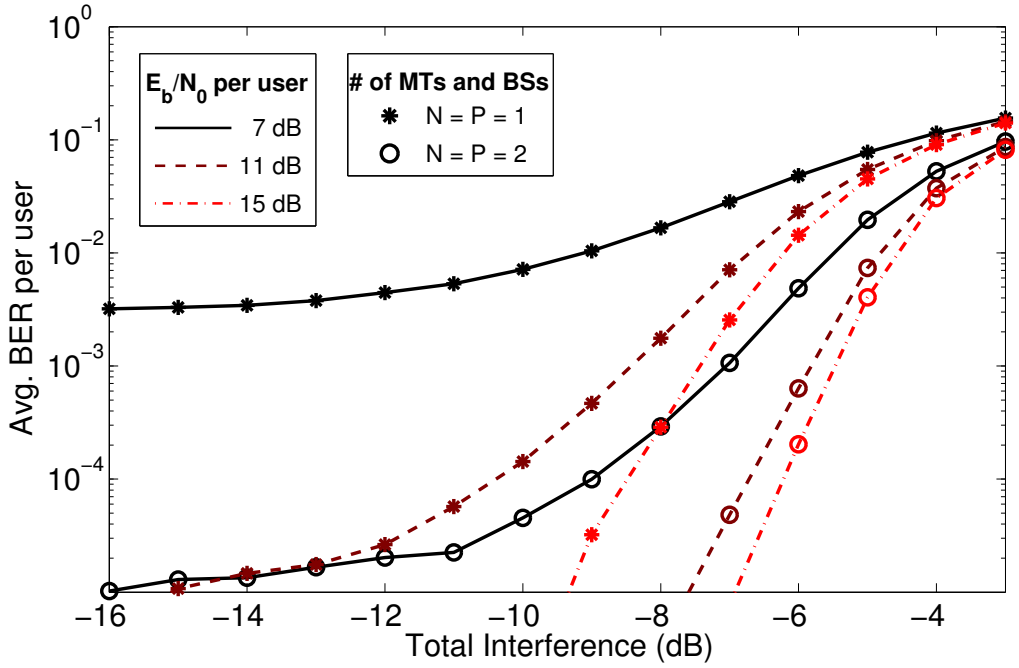

Figure 4.12: Average BER per user *vs* total interference for the 4th iteration of IB-DFE, considering both the case with BS cooperation and the one without.

4.2.3 Final Comments

Wrapping up the performance results, if a power per user of at least 6dB (measured in E_b/N_0) is considered, it is clear that the total interference is the main constraint to define the effectiveness of this system. This constraint is a smaller problem if LDPC coding and turbo equalization are used and, in this situation, if the interference is small enough, the

power per user can be very low. Nevertheless, it will always outperform his equivalent without the BS cooperation.

All this is done without creating any additional effort to the MTs, at the expense of some extra computational power at the BSs. Indeed, if some effort is made in order to pair up in the same physical channel the MTs sharing the same cell edges, while trying to minimize the interference observed for those MTs, by assigning that same frequency band to other MTs as far away as possible from the receiving BSs, it is easily possible to achieve phenomenal gains.

4.3 Improved Spectral Efficiency with Clustering

While MU-MIMO IB-DFE is a fantastic mean to improve the spectral efficiency, given that the receiver has at least as many antennas as the number of signals it's trying to detect, it is not possible to apply in all situations. Firstly, the multiple user IB-DFE cannot successfully isolate and detect signals whose power is considerably inferior to the other signals sharing the physical channel, rendering most of the usefulness of the algorithm to users with similar power levels. Secondly, given that each IB-DFE iteration requires several matrix inversions, being the matrices square and with the size equal to the number of signals to be detected, the computational complexity increases exponentially with the size of the system. In the multiple user scenario, the IB-DFE is then limited to a small size of MTs, standing close to each other in a single cluster.

Considering the aforementioned constraints, this section aim to expand the utility of the multiple user IB-DFE through a clustered multi-user detection. After a given cluster of users is resolved, using the multiple user IB-DFE, it is possible to remove that cluster's interference at the receiver, using both the channel's and the signal's estimations. The resulting signal is then composed by the channel noise plus any detection mistakes from the previous steps which, hopefully, are negligible. This means it is possible to add and resolve another cluster of MTs, on the same physical channel, as long as their signals don't interfere with the first cluster. For the IB-DFE, this is possible if the second cluster has considerably less power than the first cluster, while being high enough to be detectable through the IB-DFE. To decrease this undesired power difference limitation, once again channel coding [39] and a turbo equalization configuration [10] can be used, improving the receiver's performance and, therefore, reducing the interference effect [10].

4.3.1 Clustered Multi-user Detection Through IB-DFE

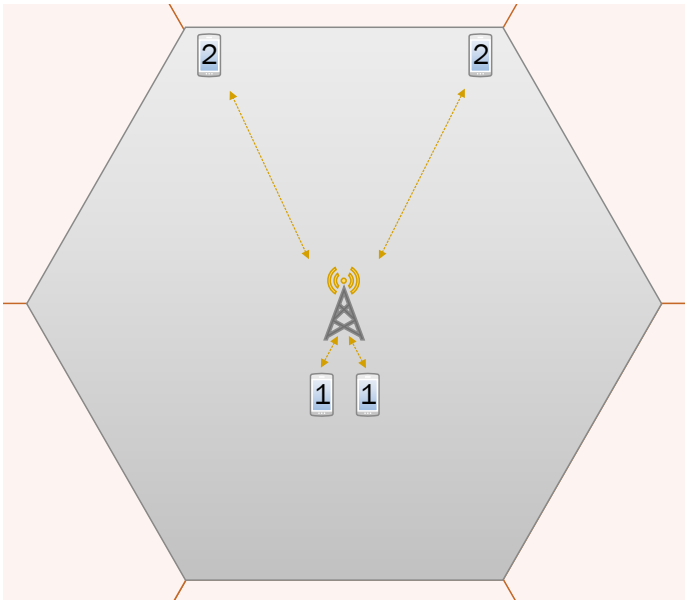

Figure 4.13: System representation, with $N = 2$ and $P = 4$. The MTs with 1 belong to the closer cluster and the MTs with 2 belong to the distant one. It is considered that all MTs are using the same physical channel.

This section will describe how and why the IB-DFE algorithm should be employed to systems as represented in Fig. 4.13. From the general equation (3.7), a clustered version can be created, represented by

$$\mathbf{S}_k = \begin{bmatrix} \mathbf{S1}_k{}^T & \mathbf{S2}_k{}^T \end{bmatrix}^T, \tag{4.9}$$

where

$$\mathbf{S1}_k = \begin{bmatrix} S_{k,(1)} & \cdots & S_{k,(P_1)} \end{bmatrix}^T \tag{4.10}$$

and

$$\mathbf{S2}_k = \begin{bmatrix} S_{k,(P_1+1)} & \cdots & S_{k,(P_1+P_2)} \end{bmatrix}^T, \tag{4.11}$$

being P_1 and P_2 the size of clusters 1 and 2, respectively, with $P_1 + P_2 = P$. $\mathbf{S1}_k$ and $\mathbf{S2}_k$ are then column vectors containing the k-th DFT values of their cluster's transmitted signals. In a similar fashion, $\mathbf{H}_k$ can also be represented in a clustered version, as shown in equations (4.12)-(4.14).

$$\mathbf{H}_k = \begin{bmatrix} \mathbf{H1}_k & \mathbf{H2}_k \end{bmatrix}, \tag{4.12}$$

$$\mathbf{H1}_k = \begin{bmatrix} H^{(1)}_{k,(1)} & \cdots & H^{(1)}_{k,(P_1)} \\ \vdots & \ddots & \vdots \\ H^{(N)}_{k,(1)} & \cdots & H^{(N)}_{k,(P_1)} \end{bmatrix} \tag{4.13}$$

$$\mathbf{H}2_k = \begin{bmatrix} H^{(1)}_{k,(P_1+1)} & \cdots & H^{(1)}_{k,(P_1+P_2)} \\ \vdots & \ddots & \vdots \\ H^{(N)}_{k,(P_1+1)} & \cdots & H^{(N)}_{k,(P_1+P_2)} \end{bmatrix} \tag{4.14}$$

With the clustered notation in mind, equation (3.9) can be rewritten as

$$\mathbf{Y}_k = \mathbf{H}1_k\mathbf{S}1_k + \mathbf{H}2_k\mathbf{S}2_k + \mathbf{N}_k = \mathbf{H}1_k\mathbf{S}1_k + \mathbf{N}1_k, \tag{4.15}$$

where

$$\mathbf{N}1_k = \mathbf{H}2_k\mathbf{S}2_k + \mathbf{N}_k. \tag{4.16}$$

Equation (4.15) sets forth the next step. As was shown, cluster 1 can be isolated and detected performing a regular IB-DFE, if cluster 2 is considered as added noise. As $\mathbf{S}2_k$ is totally unknown at this point and it is independent of $\mathbf{N}_k$, the total noise's power ($E\{|\mathbf{N}1_k|^2\}$) is the sum of the individual components' power (i.e., $E\{|\mathbf{H}2_k\mathbf{S}2_k|^2\} + E\{|\mathbf{N}_k|^2\}$).

As result of the previous step, a hard estimation of $\mathbf{S}1_k$, $\widehat{\mathbf{S}}1_k$, is obtained. As the channel response and the signal estimation are known, it is possible to mitigate cluster 1's effect on the received signal, as shown in following equation. The prevalent signal at the receiver would then be cluster 2.

$$\mathbf{Y}2_k = \mathbf{Y}_k - \mathbf{H}1_k\widehat{\mathbf{S}}1_k = \mathbf{H}2_k\mathbf{S}2_k + \mathbf{N}2_k, \tag{4.17}$$

where

$$\mathbf{N}2_k = \mathbf{N}_k + \mathbf{H}1_k(\mathbf{S}1_k - \widehat{\mathbf{S}}1_k). \tag{4.18}$$

Once again, equation (4.17) demonstrates the possibility of performing another IB-DFE, this time to isolate and detect cluster 2. However, this time the considered noise will be the sum of two independent contributors. The first and obvious one, is the channel noise, $\mathbf{N}_k$. The second one is the estimation error due to the imperfect estimation of cluster 1. The accuracy of the hard estimation $\widehat{\mathbf{S}}1_k$ is a crucial factor for the overall performance, given its influence on the considered noise power. Knowing that $\mathbf{N}_k$ and $\mathbf{H}1_k$ are uncorrelated with each other and uncorrelated with $\mathbf{S}1_k$ or $\widehat{\mathbf{S}}1_k$, we can easily find $\mathbf{N}2_k$'s power, given by

$$E\{|\mathbf{N}2_k|^2\} = E\{|\mathbf{N}_k|^2\} + E\{|\mathbf{H}1_k|^2\}E\{|(\mathbf{S}1_k - \widehat{\mathbf{S}}1_k)|^2\}, \tag{4.19}$$

where, if we take in consideration equation (3.17) and that the power of $\widehat{\mathbf{S}}1_k$ is the same as the power of $\mathbf{S}1_k$,

$$E\{|(\mathbf{S}1_k - \widehat{\mathbf{S}}1_k)|^2\} = 2(1 - \mathbf{P}1)E\{|\mathbf{S}1_k|^2\}, \tag{4.20}$$

where $\mathbf{P}1$ is the $\mathbf{P}$ matrix for the first cluster's IB-DFE.

4.3.2 IB-DFE Iteration Order for Clustered Multi-User Detection

In the previous subsection, it was shown that the quality of the first cluster's estimation ($\widehat{\mathbf{S}}1_k$) is a key factor for the effectiveness of the second cluster's estimation ($\widehat{\mathbf{S}}2_k$). With that thought in mind, one might wonder what could be changed in order to enhance the first cluster's estimation, as it would decrease the BER for both the first and the second clusters, for the same system.

Returning to equation (4.16), it is clear that if the second cluster's signals have more power at the receiver that the channel noise (which is safe to assume, if we desire a reliable communication for this cluster), the noise seen by the first cluster is dominated by those second cluster's signals. If a estimation of the second cluster is known (i.e. after at least one IB-DFE iteration for the second cluster), it is then possible to reduce the noise seen by the first cluster, following the same logic as equations (4.17)-(4.20). As the channel matrix for the second cluster ($\mathbf{H}2_k$) is independent of that cluster's signal and correspondent estimation ($\mathbf{S}2_k$ and $\widehat{\mathbf{S}}2_k$), the noise seen by the first cluster would have a power given by

$$E\{|\mathbf{N}1_k|^2\} = E\{|\mathbf{N}_k|^2\} + E\{|\mathbf{H}2_k|^2\}E\{|(\mathbf{S}2_k - \widehat{\mathbf{S}}2_k)|^2\}, \tag{4.21}$$

where

$$E\{|(\mathbf{S}2_k - \widehat{\mathbf{S}}2_k)|^2\} = 2(1 - \mathbf{P}2)E\{|\mathbf{S}2_k|^2\}. \tag{4.22}$$

Given unlimited IB-DFE iterations alternating between both clusters, it is theoretically possible to greatly reduce the noise seen by each cluster, yielding remarkable results. However, one of this clustered scheme's goals is to keep the complexity level and the computational needs bellow the standard IB-DFE. Even so, results prove that the overall performance is increased if the iterative block decision feedback equalization (IB-DFE) iterations between clusters are alternated (in certain orders, as seen below), while maintaining the total number of IB-DFE iterations. This means that even a imperfect estimation of the second cluster can make a difference for the first cluster's estimation, which in turn allows for a better final estimation of the second cluster.

4.3.3 Simulations Results

In order to compare different power configurations between the clusters, it is considered $P = 4$ users (split evenly in 2 clusters) and $N = 2$ receiving antennas for the default scenario. For the IB-DFE algorithm, the considered the results came after the 4th iteration, a point from which further iterations do not yield meaningful performance improvement [9]. All the remaining simulation set-up parameters remain the same as in 4.1.3.

In Fig. 4.14, the aforementioned scheme is simulated for various levels of power per user from the close cluster, while varying the power difference between clusters. Please note that the power difference between clusters is stated as a negative value so as to facilitate the interpretation, as the power per distant cluster's user increases from the left to the right. As it can be observed, in order to obtain a good BER level for the close cluster (let's consider it 10^{-4}), the distant cluster must have a power level at least 6dB smaller. This is considering that the users from the close cluster have a high power level, a requirement for the successful detection of all the desired signals. For the distant cluster, we have two constraints needed to be fulfilled in order to obtain a good BER level. Firstly, as discussed previously, any mistake from the close cluster's detection passes over to the distant cluster's signals as a considerable amount of noise, given their power difference. Secondly, the distant cluster still needs to be powerful enough when compared to the channel noise, otherwise the IB-DFE algorithm won't be able to perform a successful detection. To satisfy this two conditions, each user from the distant cluster should have at least around 13dB[4] of E_b/N_0, while being at least 6dB less powerful than the users from the close cluster.

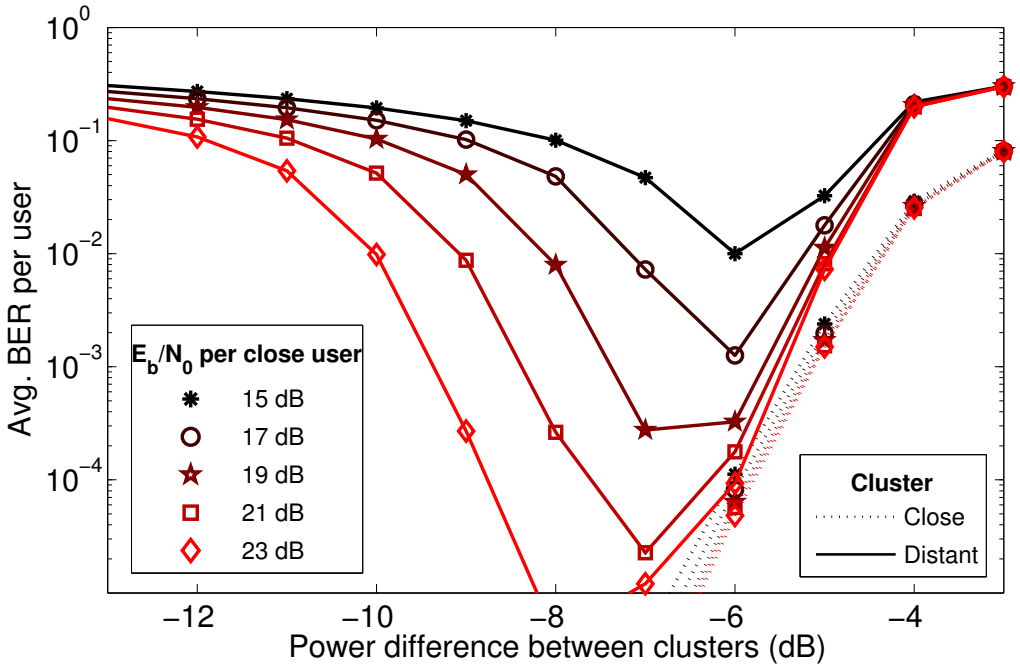

Figure 4.14: Average BER per user *vs* power difference between clusters for the 4th iteration of IB-DFE on each cluster, considering various values for the power per user in the close cluster.

Adding on extra receiving antenna to the previous scenario yields the results shown in Fig. 4.15. For the close cluster, the minimum power difference allowed for the same

[4] E_b/N_0 per close user + Power difference between clusters

considered BER level has decreased by 1dB, to 5dB. For the distant cluster, there were greater improvements. The minimum power required per distant user became around 10dB of E_b/N_0 and the minimum power difference required has decreases to up to 4dB. Of course, if we have 4dB of power difference between clusters the close cluster would have a poor BER performance, so we should look forward to fulfill both power difference requirements, 5dB. Attaching one extra antenna to the receiving system allows for lower power requirements, at the expense of extra computational power via extra feedforward coefficients.

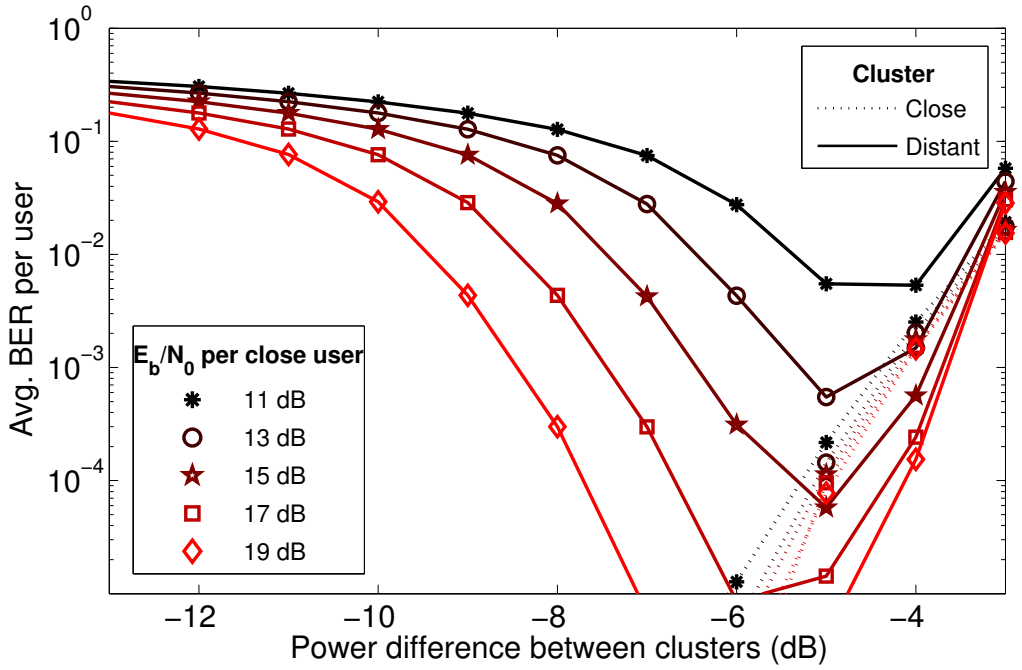

Figure 4.15: Average BER per user *vs* power difference between clusters for the 4th iteration of IB-DFE on each cluster with one extra receiving antenna ($N = 3$), considering various values for the power per user in the close cluster.

Fig. 4.16 is obtained by applying LDPC coding with a code rate of $1/2$ and turbo equalization to a scenario similar to the first set of results. While the close cluster managed to develop a certain immunity towards the interference from the distant cluster, with a BER of at most 10^{-4} for power differences up to almost 2dB, the performance bottleneck comes from the distant closer. For a good BER performance it is required that the distant cluster has at least 10dB of E_b/N_0 per user, with a power difference of 4.6dB between clusters. Even though this scheme allows for lower absolute power values and has a lower BER for optimal conditions, it is interesting to realize that the minimum requirements for a BER of 10^{-4} on both clusters are similar to previous simulated scenario.

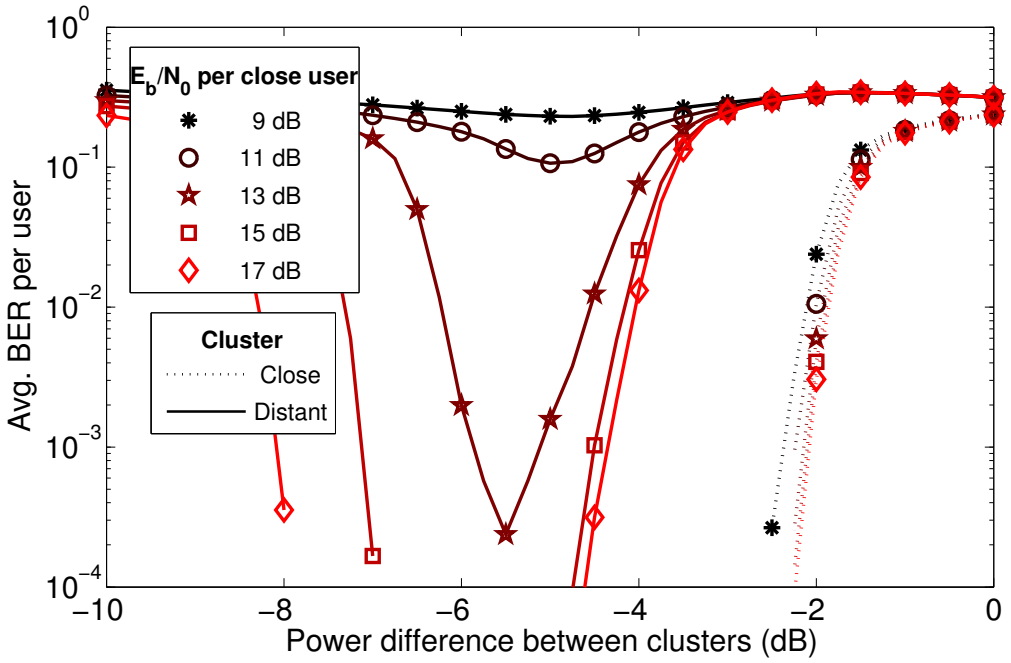

Figure 4.16: Average BER per user *vs* power difference between clusters for the 4th iteration of a turbo IB-DFE on each cluster, using LDPC coding with a rate of 0.5 and considering various values for the power per user in the close cluster.

Finally, a performance comparison between the different iteration sequences is represented in Fig. 4.17. For this comparison we've considered a power per close cluster's user of 21dB of E_b/N_0 but, from our other simulations, the same conclusions can be drawn for any chosen power level. We considered a total of 4 IB-DFE iterations per cluster and 4 possible configurations, as described in table 4.1. Configuration 4 does indeed improve considerably our scheme's overall performance, both for the close and the distant clusters. For this specific simulated scenario, not only the minimum power difference between clusters for a BER of 10^{-4} on both clusters has decreased by about 0.5dB, but also the BER on the optimal region is greatly improved.

Table 4.1: Table with the considered iteration sequences

Config.	Description
1	Intercalated iterations between clusters, 1 by 1
2	Intercalated iterations between clusters, 2 by 2
3	4 iterations on the close cluster followed by 4 on the distant one (original configuration)
4	3 iterations on the close cluster, 3 on the distant one and then 1 additional iteration on each cluster

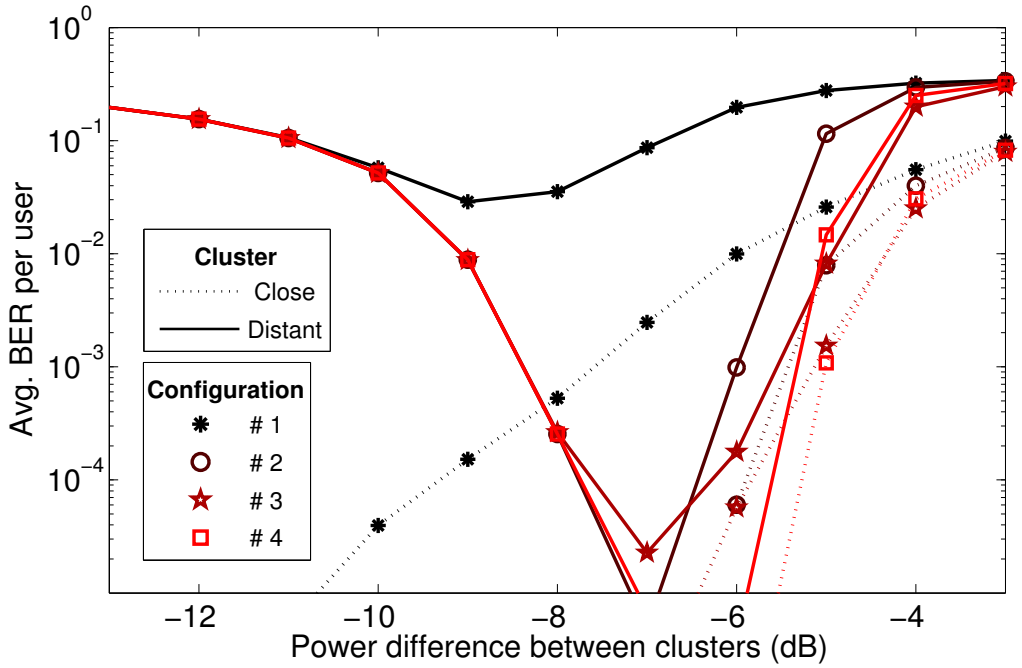

Figure 4.17: Average BER per user *vs* power difference between clusters for the 4th iteration of IB-DFE on each cluster, considering various iteration orders.

4.3.4 Final Comments

On this section, it is considered a new approach for cluster-based detection, allowing for two separate groups of users to be successfully detected while sharing the same physical channel. Both computational effort and the number of receiving antennas required by the base station are reduced, if compared to the detection of all MTs in a single IB-DFE run, and no change was needed regarding the MTs' transmission. As for the power levels required, they are not too demanding and can be eased by a set of simple techniques. It is then an impressive, yet simple mean to improve overall spectral efficiency in a multiple user scenario, given that there are clusters (of users) with power differences between them.

5

Conclusions

Contents

Throughout this thesis, the potential of a MIMO systems combined with IB-DFE for uplink communications has been studied. With their enhanced spectral efficiency, MIMO systems are undoubtedly a key element for the future of wireless and mobile communications. However, their higher capabilities come with burdensome cost: to fully extract the promised potential, complex signal separation and equalization algorithms must be employed. Given its highest potential amongst the uplink MIMO SC FD equalizers, the IB-DFE algorithm was chosen. Even with this computationally demanding algorithm, the minimum power requirements to achieve a decent BER level for the desired throughput can be a barrier for MIMO implementations, especially in multiple-users scenarios (MU-MIMO).

This work focused then in removing some of the aforementioned barriers through signal processing. To do so, three independent solutions are proposed, whose results were discussed with detail in chapter 4. The magnitude modulation solution, while already existing for SISO systems, turned out to yield considerable results especially when combined with turbo IB-DFE implementations. It is thus a major asset to any MIMO or MU-MIMO system. The base station cooperation scheme showed us that, when combined MU-MIMO IB-DFE systems, the overall performance for users at cell edges can improve greatly. This is of utmost importance, since those specific users usually struggle to get a good performance. Finally, a cluster-based multi-user detection scheme demonstrated that is possible to double the spectral efficiency of a given MU-MIMO system without introducing a computational complexity exponentially bigger. While it has some power-level related requirements, if those requirements are met it is possible to greatly improve the global system's throughput.

5.1 Future Work

Even though positive results were obtained in this thesis, several assumptions were made. MIMO system's transmitting antennas can have different power levels between themselves and MU-MIMO users grouped together might have slightly different power levels at the receiver. Also, MIMO systems have several configurations regarding the number of antennas used, MM techniques can be applied more than once per transmitted block, base station cooperation schemes can use more than 2 cooperating BSs and the cluster-based multi-user detection can attempt to detect a third cluster on the same physical channel. For a fully realistic evaluation of the proposed techniques, a complete generalization must be performed.

Bibliography

[1] C. Systems, "Cisco Visual Networking Index: Global Mobile Data Traffic Forecast Update, 2013–2018," http://www.cisco.com/c/en/us/solutions/collateral/service-provider/visual-networking-index-vni/white_paper_c11-520862.html, Feb 2014.

[2] M. Di Renzo, H. Haas, A. Ghrayeb, S. Sugiura, and L. Hanzo, "Spatial modulation for generalized mimo: Challenges, opportunities, and implementation," *Proceedings of the IEEE*, vol. 102, no. 1, pp. 56–103, Jan 2014.

[3] C. E. Shannon, *A Mathematical Theory of Communications*. Bell Systems Technical Journal, 1948, vol. 27.

[4] M. Dohler, R. Heath, A. Lozano, C. Papadias, and R. Valenzuela, "Is the phy layer dead?" *IEEE Comm. Mag.*, vol. 49, no. 4, pp. 159–165, Apr 2011.

[5] G. Foschini and M. Gans, "On limits of wireless communications in a fading environment when using multiple antennas," *Wireless Pers. Commun.*, vol. 6, no. 3, pp. 311–335, March 1998.

[6] E. Telatar, "Capacity of multiantenna gaussian channels," *European Transactions on Telecommunications*, vol. 10, no. 6, pp. 585–595, Dec 1999.

[7] G. J. Foschini, "Layered space-time architecture for wireless communication in a fading environment when using multi-element antennas," *Bell Labs Technical Journal*, vol. 1, no. 2, pp. 41–59, Autumn 1996.

[8] N. Benvenuto and S. Tomasin, "Block iterative dfe for single carrier modulation," *Electron. Lett.*, vol. 39, no. 19, pp. 1144–1145, September 2002.

[9] R. Dinis, R. Kalbasi, D. Falconer, and A. Banihashemi, "Iterative layered space-time receivers for single-carrier transmission over severe time-dispersive channels," *IEEE Comm. Letters*, vol. 39, no. 19, pp. 1144–1145, September 2004.

[10] N. Benvenuto, R. Dinis, D. Falconer, and S. Tomasin, "Single carrier modulation with nonlinear frequency domain equalization: An idea whose time has come again," *Proceedings of the IEEE*, vol. 98, no. 1, pp. 69–96, jan. 2010.

[11] D. Gesbert, D. Hanly, H. Huang, S. Shitz, O. Simeone, and W. Yu, "Multi-cell mimo cooperative networks: A new look at interference," *IEEE JSAC*, vol. 28, no. 9, pp. 1380–1408, Dec 2010.

[12] F. Casal Ribeiro, R. Dinis, F. Cercas, and A. Silva, "Iterative frequency-domain receivers for the uplink of cellular systems with base station cooperation," *IEEE CN'2012*, Aug 2012.

[13] ——, "Analytical performance evaluation of base station cooperation systems using sc-fde modulations with iterative receivers," *IEEE Globecom Workshops*, pp. 637–641, Dec 2012.

[14] J. Gante, M. Gomes, R. Dinis, V. Silva, and F. Cercas, "Power efficient mimo sc-fde transmission using magnitude modulation techniques," *IEEE 80th Vehicular Technology Conference: VTC2014-Fall*, Sep 2014.

[15] ——, "Towards an enhanced frequency reuse: Uplink base station cooperation with iterative receivers and ldpc coding," *IEEE 81th Vehicular Technology Conference: VTC2015-Spring*, 2015 (submitted paper).

[16] ——, "Clustered multiuser detection using sc-fde transmission with iterative receivers," *IEEE ICC'15*, 2015 (submitted paper).

[17] E. Biglieri, *MIMO Wireless Communication*. Cambridge University Press, 2007.

[18] A. Carlson and P. Crilly, *Communication Systems*. McGraw-Hill, 2009.

[19] C. Langton, "Finding MIMO ," http://complextoreal.com/wp-content/uploads/2013/01/mimo.pdfl, Oct 2011.

[20] C. Tidestav, M. Sternad, and A. Ahlen, "Reuse within a cell-interference rejection or multiuser detection?" *Communications, IEEE Transactions on*, vol. 47, no. 10, pp. 1511–1522, Oct 1999.

[21] N. Al-Dhahir and A. Sayed, "The finite-length multi-input multi-output mmse-dfe," *Signal Processing, IEEE Transactions on*, vol. 48, no. 10, pp. 2921–2936, Oct 2000.

[22] A. Lozano and C. Papadias, "Layered space-time receivers for frequency-selective wireless channels," *Communications, IEEE Transactions on*, vol. 50, no. 1, pp. 65–73, Jan 2002.

[23] D. Falconer, S. Ariyavisitakul, A. Benyamin-Seeyar, and B. Eidson, "Frequency domain equalization for single-carrier broadband wireless systems," *Communications Magazine, IEEE*, vol. 40, no. 4, pp. 58–66, Apr 2002.

[24] A. Gurmão, R. Dinis, J. Conceição, and N. Esteves, "Comparison of two modulation choices for broadband wireless communications," *Proc. IEEE VTC'00(Spring)*, vol. 2, pp. 1300–1305, May 2000.

[25] G. Quan, J. Yan-liang, S. Zhi-dong, and M. Hui-jun, "Papr analysis for single-carrier fdma mimo systems with space-time/frequency block codes," in *Networks Security Wireless Communications and Trusted Computing (NSWCTC), 2010 Second International Conference on*, vol. 2, April 2010, pp. 126–129.

[26] P. Silva and R. Dinis, *Frequency-Domain Multiuser Detection for CDMA Systems*. River Publishers, 2012.

[27] R. Dinis, A. Gusmão, and N. Esteves, "On broadband block transmission over strongly frequency-selective fading channels," in *IEEE Wireless'03*, Calgary, Canada, July 2003.

[28] N. Benvanuto and G. Cherubini, *Algorithms for Communications Systems and Their Applications*. Chichester, U.K.: Wiley, 2002.

[29] M. Gomes, V. Silva, F. Cercas, and M. Tomlinson, "Power efficient back-off reduction through polyphase filtering magnitude modulation," *IEEE Commun. Lett.*, vol. 13, no. 8, pp. 606–608, August 2009.

[30] M. Gomes, R. Dinis, V. Silva, F. Cercas, and M. Tomlinson, "Error rate analysis of m-psk with magnitude modulation envelope control," *Electronics Letters*, vol. 49, no. 18, pp. 1184–1186, August 2013.

[31] ——, "Iterative frequency domain equalization for single carrier signals with magnitude modulation techniques," in *IEEE 76th Vehicular Technology Conference: VTC2012-Fall*, Québec City, Canada, September 2012.

[32] ——, "Iterative fde design for ldpc-coded magnitude modulation schemes," in *Wireless Communication Systems (ISWCS 2013), Proceedings of the Tenth International Symposium on*, Aug 2013, pp. 1–5.

[33] S. Miller and R. O'Dea, "Peak power and bandwidth efficient linear modulation," *IEEE Trans. Commun.*, vol. 46, no. 12, pp. 1639–1648, Dec. 1998.

[34] M. Gomes, "Magnitude modulation for peak power control in single carrier communication systems," Ph.D. dissertation, Universidade de Coimbra, Portugal, 2010.

[35] A. Ambroze, M. Tomlinson, and G. Wade, "Magnitude modulation for small satellite earth terminals using qpsk and oqpsk," in *Communications, 2003. ICC '03. IEEE International Conference on*, vol. 3, May 2003, pp. 2099–2103 vol.3.

[36] M. Tomlinson, A. Ambroze, and G. Wade, "Power and bandwidth efficient modulation and coding for small satellite communication terminals," *Proc. IEEE ICC'02*, vol. 5, pp. 2943–2946, Apr. 2002.

[37] A. Gusmão, R. Dinis, and N. Esteves, "On frequency-domain equalization and diversity combining for broadband communications," *IEEE Trans. Commun.*, vol. 51, pp. 1029–1033, July 2003.

[38] T. Mayer, H. Jenkac, and J. Hagenauer, "Turbo base-station cooperation for intercell interference cancellation," *IEEE ICC'06*, 2006.

[39] S. Lin and J. D. J. Costello, *Error Control Coding, 2nd ed.* NJ: Pearson Prentice Hall, 2004.

Accepted Paper at IEEE VTC2014-Fall

Power Efficient MIMO SC-FDE Transmission using Magnitude Modulation Techniques

João Gante*†, Marco Gomes*†, Rui Dinis*‡, Vitor Silva*† and Francisco Cercas*§
*Instituto de Telecomunicações, Portugal
†Department of Electrical and Computer Engineering, University of Coimbra, 3030-290 Coimbra, Portugal
‡FCT-UNL, 2829-516 Caparica, Portugal, §ISCTE-IUL, 1649-026 Lisbon, Portugal

***Abstract*—Polyphase magnitude modulation (MM) has been shown to be a robust and effortless mean to improve the efficiency of a transmitter's high power amplifier (HPA), due to the real-time reduction of the peak to average power ratio (PAPR). MM's technique flexibility allows us to include the MM system on any existing single-carrier (SC) based transmission system with clear benefits on the achieved bit error rate *vs* overall signal power to noise ratio.**

This paper analyzes the efficiency of MM when added to a multi-input multi-output (MIMO) system, using a block-based SC transmission combined with iterative block decision feedback equalization (IB-DFE). To improve the IB-DFE performance for low power signals, we consider an additional scheme where low-density parity-check (LDPC) coding and turbo equalization are added. Simulation results show a net power efficiency enhancement, particularly for systems with channel coding, confirming MM as a major asset for high performance communication systems.

I. Introduction

In the current human society, we aim to achieve higher and higher data throughput. For mobile users, another objective arises — energy efficiency [1], [2]. As a mobile user, we demand a huge amount of data with a very limited energy source, meaning that power efficiency is a key element for modern telecommunications.

To address the first issue, it has been proved [3] that a multi-input multi-output (MIMO) scheme is a very powerful tool to improve the usage of the physically limited bandwidth. By employing multiple antennas at both the transmitter and receiver, we are able to greatly improve the spectral efficiency, either by increasing the channel diversity or by using space-time multiplexing [4], [5].

However, mobile environment systems may also deal with inter-carrier and inter-symbol interference due to the strong dispersive nature of the channel. From this perspective, MIMO systems can be combined with popular block-based transmission techniques particularly suited for communication over severe time-dispersive channels by employing low complexity frequency domain equalisation (FDE) [6]. Popular techniques are orthogonal frequency domain multiplexing (OFDM) [7] and single-carrier with frequency domain equalisation (SC-FDE) [6], the latter being of special interest at the uplink transmission given the low peak-to-average power ratio (PAPR) [8] and the possibility of replacing the conventional linear FDE by a non-linear FDE such as the iterative-block decision feedback equaliser (IB-DFE) [9], with significant gains in performance.

It was shown in previous works [10], [11] that the use of SC-FDE combined with IB-DFE on a MIMO system results on the desired higher spectral efficiency, while coping with severe time-dispersion, with simple changes to the classical IB-DFE scheme [9]. At the transmitter, the data stream is multiplexed into P blocks (layers), each one with the same length, which are simultaneously transmitted over P antennas. Considering a frequency-domain iterative receiver with at least as many antennas as the transmitter, the aforementioned IB-DFE method [11] allows to eliminate simultaneously time-dispersion interference as well as a significant part of the interlayer interference.

Although, one of MIMO's greatest potential is it's usage on mobile terminals, they still suffer from energy starvation, given their power hungry high power amplifiers (HPAs) and limited batteries. A great way to improve the efficiency of SC based systems is to perform polyphase magnitude modulation [12], [13] of the signal to transmit. By trying to suppress peaks from the transmitted signals, we are able to reduce the PAPR, which reduces the HPA's back-off. Results have shown that between BER performance losses and power efficiency gains from the reduced HPA's back-off, we have a high net power gain, even for severe time-dispersive scenarios [14]. MM creates then the possibility to transmit more power while delivering the same maximum power to the HPA, with very little computational effort. It was also shown that these results can be improved using channel coding, which reduces the BER performance losses [12], [15].

In this paper, we propose to combine MM techniques with MIMO systems for SC-FDE transmissions with IB-DFE equalization at the reception. By controlling the envelope of the signal fed to each transmitting antenna through MM, we can considerably increase the power efficiency of the HPAs. To obtain a complete insight of the whole scheme, we simulate both uncoded and coded transmission system, with the later using LDPC coding [16] and a turbo equalization configuration [9]. The first system was designed to confirm our

This work was supported in part by the Instituto de Telecomunicações and in part by the Fundação para a Ciência e Tecnologia under projects: PEst-OE/EEI/LA0008/2013 (P01229 - GLANCES), GALNC (EXPL/EEI-TEL/1582/2013) and ADIN (PTDC/EEI-TEL/2990/2012).

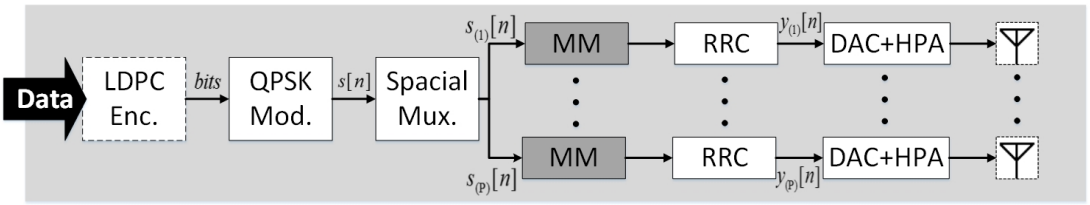

Fig. 1. General diagram of the proposed transmitter.

studies about how effective MM is and how well it works in cooperation with more sophisticated systems like MIMO with IB-DFE. To further improve our system (and to get closer to modern wireless communication systems), we added coding and upgraded our scheme with turbo equalization, making changes on the information that was fed back in every IB-DFE iteration. This greatly improves IB-DFE performance for low signal-to-noise ratio (SNR) signals, where the coding scheme has its most meaningful work, while suppressing the MM BER losses. The results of this combined system far surpass the original techniques' (MM with channel coding [12] and turbo equalization [9]) individually.

This paper is organized as follows: the basic scheme is described in Section 2. Improvements to that scheme are proposed in Section 3. A set of performance results is presented in Section 4 and Section 5 is concerned with the conclusions.

II. MIMO WITH IB-DFE AND MM

In the proposed scheme, we combine the receiver described in [11] with a transmission using magnitude modulation [12]. We consider a SC-FDE modulation scheme where the data is transmitted in blocks of M symbols, resulting from direct mapping of the original data bits into a selected constellation, e.g. quaternary phase shift keying (QPSK). The symbols are multiplexed into P parallel data streams $s_{(p)}[n]$ with $p = 1, \cdots, P$, as shown in Fig. 1. Each stream is magnitude modulated in order to limit the excursion of the pulse shaped signal $y_{(p)}[n]$ feed to the digital to analog converter (DAC) + HPA of antenna p, with $y_{(p)}[n]$ being given by,

$$y_{(p)}[n] = \sum_k m_{(p)}[k] s_{(p)}[k] h_{\text{RRC}}[n-k] \ , \tag{1}$$

where $h_{RRC}[n]$ is the impulse response of pulse shaping filter (typically a root-raised cosine (RRC)) and $m_{(p)}[n]$ is the MM factor applied to each symbol $s_{(p)}[n]$.

To compute $m_{(p)}[n]$ we follow the same reasoning as in [12], where we guarantee that

$$|y_{(p)}[n]|^2 \leq P_{(p),Max} \ , \tag{2}$$

with $P_{(p),Max}$ denoting the maximum admissible power at DAC + HPA of stream p. The magnitude modulated symbols are then transmitted through the P antennas, over a time dispersive channel.

At the receiver, we will attempt to recover the P different streams using the N receiving antennas, with $P \leq N$. The discussed MIMO IB-DFE [11] detects one stream at a time and cancels the interference from already detected streams, a method also known as successive interference cancellation (SIC). To maximize this method's effectiveness, it is desirable to rank the streams according to some quality measure (we use the average received power) and to detect the streams from the best to the worst. Hence, the interference of the strongest stream is diminished when we're attempting to detect the weakest one, which proves to be very difficult otherwise. At the same time the IB-DFE system works on interference cancellation, by employing frequency domain equalization, with both feedback and feedforward filters. The algorithm works on a per-block basis, meaning that the feedback's effectiveness to cancel all the interferences is limited by the reliability of the detected data at previous iterations. Consequently, it is usually desired to apply more than one iteration per block.

Let the time-domain blocks at the pth transmitting antenna and nth receiving antenna be respectively

$$\mathbf{s}_{(p)} = \left[s_{1,(p)} \cdots \ s_{M,(p)} \right]^T \tag{3}$$

and

$$\mathbf{y}^{(n)} = \left[y_1^{(n)} \cdots \ y_M^{(n)} \right]^T \ , \tag{4}$$

with $n = 1, \cdots, N$, and let

$$\mathbf{S}_{(p)} = \left[S_{1,(p)} \cdots \ S_{M,(p)} \right]^T \tag{5}$$

and

$$\mathbf{Y}^{(n)} = \left[Y_1^{(n)} \cdots \ Y_M^{(n)} \right]^T \tag{6}$$

denote the M-point discrete Fourier transforms (DFT) of $\mathbf{s}_{(p)}$ and $\mathbf{y}^{(n)}$, where

$$S_{k,(p)} = \sum_{m=0}^{M-1} s_{m,(p)} e^{(-j2\pi km/M)} \tag{7}$$

and

$$Y_k^{(n)} = \sum_{m=0}^{M-1} y_m^{(n)} e^{(-j2\pi km/M)} \ . \tag{8}$$

Being $\mathbf{S}_k$ and $\mathbf{Y}_k$ the N-tuple vectors of the obtained DFT coefficients for each k sub-carrier, with $k = 0, \cdots, M-1$, given by

$$\mathbf{S}_k = \left[S_{k,(1)} \cdots \ S_{k,(P)} \right]^T \tag{9}$$

and

$$\mathbf{Y}_k = \left[Y_k^{(1)} \cdots \ Y_k^{(N)} \right]^T \ , \tag{10}$$

the receiving frequency-domain signal $\mathbf{Y}_k$ can be written as

$$\mathbf{Y}_k = \mathbf{H}_k \mathbf{S}_k + \mathbf{N}_k \ , \tag{11}$$

where, $\mathbf{H}_k$ and $\mathbf{N}_k$ represent respectively the frequency-domain dispersive channel and additive white gaussian noise (AWGN) matrices, written as

$$\mathbf{H}_k = \begin{bmatrix} H^{(1)}_{k,(1)} & \cdots & H^{(1)}_{k,(P)} \\ \vdots & \ddots & \vdots \\ H^{(N)}_{k,(1)} & \cdots & H^{(N)}_{k,(P)} \end{bmatrix} \tag{12}$$

and

$$\mathbf{N}_k = \left[N^{(1)}_k \ldots \ N^{(N)}_k \right]^T . \tag{13}$$

The frequency-domain soft-estimations associated with the pth layer at the output of the equalizer are given by

$$\widetilde{\mathbf{S}}_k = \mathbf{F}^T_k \mathbf{Y}_k - \mathbf{B}_k \widetilde{\mathbf{S}'}_k \ , \tag{14}$$

where the feedforward and feedback matrices are respectively

$$\mathbf{F}_k = \begin{bmatrix} F^{(1)}_{k,(1)} & \cdots & F^{(1)}_{k,(P)} \\ \vdots & \ddots & \vdots \\ F^{(N)}_{k,(1)} & \cdots & F^{(N)}_{k,(P)} \end{bmatrix} \tag{15}$$

and

$$\mathbf{B}_k = \begin{bmatrix} B^{(1)}_{k,(1)} & \cdots & B^{(1)}_{k,(P)} \\ \vdots & \ddots & \vdots \\ B^{(P)}_{k,(1)} & \cdots & B^{(P)}_{k,(P)} \end{bmatrix} . \tag{16}$$

$F^{(n)}_{k,(p)}$ and $B^{(p)}_{k,(p)}$ denote the feedforward and feedback filters coefficients and the vector $\widetilde{\mathbf{S}'}_k$ contains the DFT of the time-domain blocks associated with latest estimations for the transmitted symbols (for the first iteration those terms are zero).

The frequency-domain samples used in the feedback loop can produce hard-estimations, $\widehat{\mathbf{S}}_k$, which can be written as

$$\widehat{\mathbf{S}}_k = \mathbf{P}\mathbf{S}_k + \mathbf{\Delta}_k \ , \tag{17}$$

with the length-P column vector

$$\mathbf{\Delta}_k = \left[\Delta_{k,(1)} \ldots \ \Delta_{k,(P)} \right]^T , \tag{18}$$

and

$$\mathbf{P} = \mathrm{diag}(\rho_{(1)}, \ \ldots \ , \rho_{(P)}) \ . \tag{19}$$

The correlation coefficients in (19) are given by

$$\rho_{(p)} = E[S_{k,(p)} S^*_{k,(p)}]/E[|S_{k,(p)}|^2] = E[\widehat{s}_{m,(p)} s^*_{m,(p)}]/E_S \ , \tag{20}$$

where

$$E_S = E[|s_{m,(p)}|^2] = E[|S_{k,(p)}|^2]/M \tag{21}$$

is the average symbol energy, common to all layers. Since $E[\Delta_{k,(p)} S^*_{k',(p)}] \approx 0$, we have

$$E[|\Delta_{k,(p)}|^2] \approx (1 - \rho^2_{(p)}) M E_S \ . \tag{22}$$

The correlation coefficient can be estimated from the time-domain samples associated with the equalizer output, $\widetilde{s}_{m,(p)}$, as described in [17].

It can also be shown that time-domain samples associated with the equalizer output, $\widetilde{\mathbf{s}}_m$, can be written as

$$\widetilde{\mathbf{s}}_m = \mathbf{\Gamma}\mathbf{s}_m + \mathbf{E}^{eq}_m \ , \tag{23}$$

where $\mathbf{s}_m$ and $\widetilde{\mathbf{s}}_m$ denote the P size vectors with the time-domain signals and the time-domain equalizer's soft outputs, respectively. The E^{eq}_m and $\mathbf{\Gamma}$ matrices are given by

$$\mathbf{E}^{eq}_m = \left[\varepsilon^{eq}_{m,(1)} \cdots \ \varepsilon^{eq}_{m,(P)} \right]^T , \tag{24}$$

where $\varepsilon^{eq}_{m,(p)}$ denotes the overall noise plus interference, and

$$\mathbf{\Gamma} = \mathrm{diag}(\gamma) \ , \tag{25}$$

where

$$\gamma = \frac{1}{M} \sum_{k=0}^{M-1} [\mathbf{1}_{1\times N} (\mathbf{H}_k \odot \mathbf{F}_k)]^T \tag{26}$$

is a sized P column vector. The corresponding frequency-domain samples can be written as

$$\widetilde{\mathbf{S}}_k = \mathbf{\Gamma}\mathbf{S}_k + \mathbf{E}^{Eq}_k \ , \tag{27}$$

where the $\varepsilon^{Eq}_{k,(p)}$ $(k = 0, \cdots, M-1)$ terms of the P-sized vector E^{Eq}_k are the DFT of $\varepsilon^{eq}_{m,(p)}$ $(m = 0, \cdots, M-1)$. The signal to interference plus noise ratio (SNIR) in the frequency domain is written as

$$SNIR^F_{k,(p)} = \frac{|\gamma_{(p)}|^2 M E_S}{\left[|\varepsilon^{Eq}_{k,(p)}|^2 \right]} \ . \tag{28}$$

After combining (14), (28) and some algebraic manipulation, the optimum feedback coefficients that maximize (28) at a specific iteration are

$$\mathbf{B}_k = \mathbf{P}(\mathbf{F}^T_k \mathbf{H}_k - \mathbf{\Gamma}) \ . \tag{29}$$

The feedforward coefficients, required by (29) and (26), are obtained from the following equation:

$$\mathbf{F}_k = (\mathbf{I} - \mathbf{P}^2)\mathbf{\Gamma}\mathbf{H}^H_k \ [(\mathbf{I} - \mathbf{P}^2)\mathbf{H}^H_k \mathbf{H}_k + \frac{P}{SNR}\mathbf{I}]^{-1} \ , \tag{30}$$

where the SNR at each receiving antenna is

$$SNR = (PE_S)/(2\sigma^2_N) \ , \tag{31}$$

being σ^2_N the variance of the real and imaginary parts of the channel noise. Clearly, the feedforward and feedback coefficients take into account the reliability of each detected block through the corresponding correlation factor $\rho_{(p)}$. In the next section we will explore this feature, using it to further improve the system.

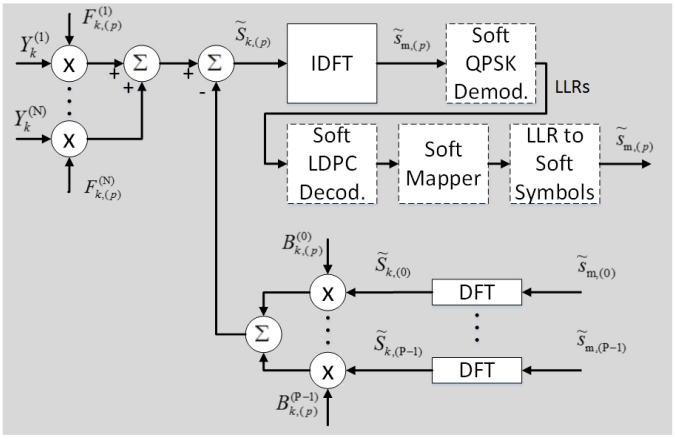

Fig. 2. Detection of the pth layer, for a given iteration in IB-DFE with turbo equalization.

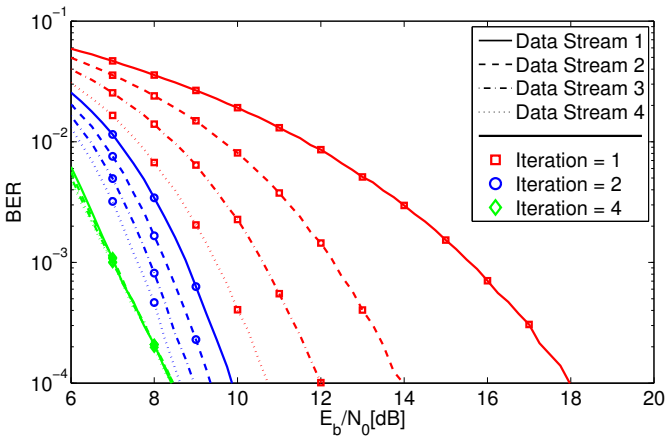

Fig. 3. BER *vs* E_b/N_0 performance of the uncoded IB-DFE with no MM, for different layers at different iterations.

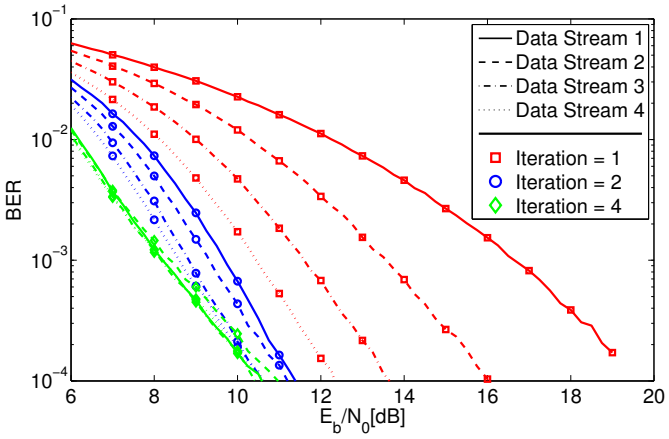

Fig. 4. BER *vs* E_b/N_0 performance of the uncoded IB-DFE with MM, for different layers at different iterations.

III. LDPC Coding and Turbo Equalization

As mentioned in [12], MM has better results when channel coding is used. The changes introduced in the time-domain symbols are quite small and a decoder can easily correct most errors, making this the first logical step to improve the proposed system.

When a MIMO IB-DFE is combined with coding/decoding, it is also called turbo equalization in the frequency domain [9]. As the new data that is fed from a block's equalization to the next is the soft estimation of the current block symbols, we can use LDPC coding [16] to obtain an improved estimation and to feed back that estimation instead. This turbo equalization has the double benefit of improving the block's estimation capacity (and therefore the correlation factor $\rho_{(p)}$, as previously discussed) and to reduce the unpleasant part of MM, the BER penalty.

For QPSK symbols with points $\{\pm 1 \pm j\}$, soft demapping and mapping is greatly simplified, becoming very easy to deploy. Defining the complex log likelihood ratio as

$$\lambda_{m,(p)} = \lambda_{R,m,(p)} + j\lambda_{I,m,(q)} \ , \tag{32}$$

where $\lambda_{R,m,(q)}$ ($\lambda_{I,m,(q)}$) is associated to $\mathrm{Re}[s_{m,(p)}]$ ($\mathrm{Im}[s_{m,(p)}]$), the soft demapper yields [18]

$$\lambda_{m,(q)} = \frac{4\widetilde{s}_{m,(p)}}{\sigma^2_{SD,(p)}} \ , \tag{33}$$

with $\sigma^2_{SD,(p)}$ being the equalizer soft output variance. This means that the log likelihood ratio is proportional to the equalizer soft output. In turn, if $\eta_{m,(p)} = \eta_{R,m,(p)} + j\eta_{I,m,(p)}$ is the complex log likelihood ratio at the decoder output (extrinsic information), we can further improve the equalizer soft output by making

$$\widetilde{s}_{m,(p))} = \tanh\left(\frac{\eta_{R,m,(p)}}{2}\right) + j\tanh\left(\frac{\eta_{I,m,(p)}}{2}\right) \ . \tag{34}$$

IV. Performance Results

In the following, we present a set of results obtained from the system's simulation. For the sake of simplicity, we will assume that our system is under perfect synchronization and channel estimation conditions.

In order to compare BER *vs* SNR performance of different layers at different iterations, we considered $P = 4$ layers and a receiver with $N = 4$ antennas. The layer's indexes indicate the order they are detected. Each layer consists of 768 QPSK data symbols, plus cyclic-extension. We considered the channel model of [19], which has uncorrelated Rayleigh fading at all frequencies (similar behaviors were observed for severe time-dispersive channels with rich multipath propagation). All layers are transmitted with the same amount of average power and when MM is used, only 1 stage is applied, considering the use of a 0.2 roll-off RRC filter.

In Figs. 3 and 4, we simulate the basic system (without LDPC coding), with and without MM. On this configuration, for the same BER, MM requires 2 dB of extra SNR. From [12], the back-off reduction is about 4.4 dB and thus we conclude

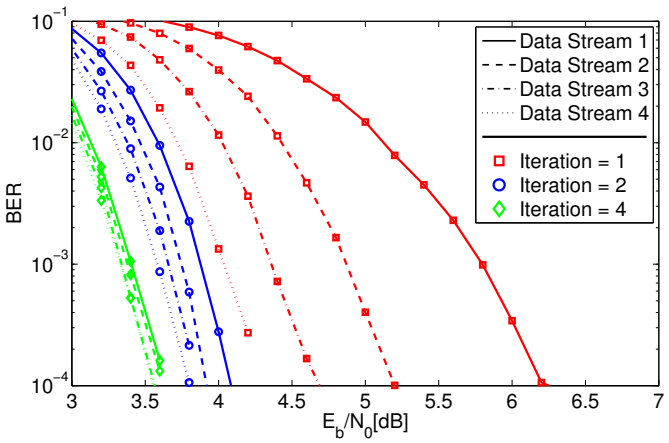

Fig. 5. BER *vs* E_b/N_0 performance of the IB-DFE with turbo equalization and no MM, for different layers at different iterations.

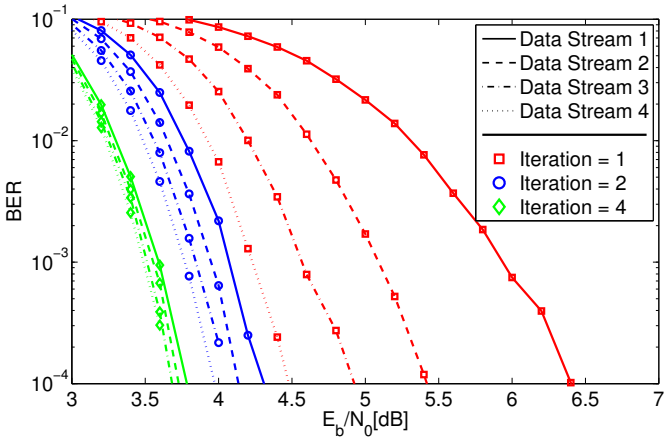

Fig. 6. BER *vs* E_b/N_0 performance of the IB-DFE with turbo equalization and MM, for different layers at different iterations.

that the system has a net gain of 2.2 dBs.

Applying a WiMAX (1536,768) LDPC code and reworking our IB-DFE algorithm towards turbo equalization greatly improved our system, as shown in figures 5 and 6. Once again, it's a comparison of the same system with and without MM. On this experiment and for the same BER, the MM only requires about 0.25 dB of extra SNR, which combined with the 4.4 dB gained from the HPA's back-off yields a net gain of 4.1 dB.

V. Conclusions

In this paper, we applied a computational-wise effortless signal processing method (MM) on a MIMO system, a system with quite a high complexity. MM can be easily applied to any currently working transmitter without any change in the receiver, providing a significant enhancement in power efficiency without interfering with the system's main function. The results obtained showed that if the system already uses coding, which always happens in modern communications, the net gain is truly remarkable.

References

[1] G. Li, Z. Xu, C. Xiong, C. Yang, S. Zhang, Y. Chen, and S. Xu, "Energy-efficient wireless communications: tutorial, survey, and open issues," *Wireless Communications, IEEE*, vol. 18, no. 6, pp. 28–35, December 2011.

[2] S. Zeadally, S. Khan, and N. Chilamkurti, "Energy-efficient networking: past, present, and future," *The Journal of Supercomputing*, vol. 62, no. 3, pp. 1093–1118, 2012.

[3] G. Foschini and M. Gans, "On limits of wireless communications in a fading environment when using multiple antennas," *Wireless Pers. Commun.*, vol. 6, no. 3, pp. 311–335, March 1998.

[4] D. Gesbert, M. Shafi, D. shan Shiu, P. Smith, and A. Naguib, "From theory to practice: an overview of mimo space-time coded wireless systems," *Selected Areas in Communications, IEEE Journal on*, vol. 21, no. 3, pp. 281–302, Apr 2003.

[5] M. Di Renzo, H. Haas, A. Ghrayeb, S. Sugiura, and L. Hanzo, "Spatial modulation for generalized mimo: Challenges, opportunities, and implementation," *Proceedings of the IEEE*, vol. 102, no. 1, pp. 56–103, Jan 2014.

[6] D. Falconer, S. Ariyavisitakul, A. Benyamin-Seeyar, and B. Eidson, "Frequency domain equalization for single-carrier broadband wireless systems," *Communications Magazine, IEEE*, vol. 40, no. 4, pp. 58–66, Apr 2002.

[7] Y. Li, J. Cimini, L.J., and N. Sollenberger, "Robust channel estimation for ofdm systems with rapid dispersive fading channels," *Communications, IEEE Transactions on*, vol. 46, no. 7, pp. 902–915, Jul. 1998.

[8] G. Quan, J. Yan-liang, S. Zhi-dong, and M. Hui-jun, "Papr analysis for single-carrier fdma mimo systems with space-time/frequency block codes," in *Networks Security Wireless Communications and Trusted Computing (NSWCTC), 2010 Second International Conference on*, vol. 2, April 2010, pp. 126–129.

[9] N. Benvenuto, R. Dinis, D. Falconer, and S. Tomasin, "Single carrier modulation with nonlinear frequency domain equalization: An idea whose time has come again," *Proceedings of the IEEE*, vol. 98, no. 1, pp. 69–96, jan. 2010.

[10] N. Benvenuto and S. Tomasin, "Block iterative dfe for single carrier modulation," *Electron. Lett.*, vol. 39, no. 19, pp. 1144–1145, September 2002.

[11] R. Dinis, R. Kalbasi, D. Falconer, and A. Banihashemi, "Iterative layered space-time receivers for single-carrier transmission over severe time-dispersive channels," *IEEE Comm. Letters*, vol. 39, no. 19, pp. 1144–1145, September 2004.

[12] M. Gomes, V. Silva, F. Cercas, and M. Tomlinson, "Power efficient back-off reduction through polyphase filtering magnitude modulation," *IEEE Commun. Lett.*, vol. 13, no. 8, pp. 606–608, August 2009.

[13] M. Gomes, R. Dinis, V. Silva, F. Cercas, and M. Tomlinson, "Error rate analysis of m-psk with magnitude modulation envelope control," *Electronics Letters*, vol. 49, no. 18, pp. 1184–1186, August 2013.

[14] M. Gomes, R. Dinis, V. Silva, F. Cercas, and M. Tomlinson, "Iterative frequency domain equalization for single carrier signals with magnitude modulation techniques," in *IEEE 76th Vehicular Technology Conference: VTC2012-Fall*, Québec City, Canada, September 2012.

[15] M. Gomes, R. Dinis, V. Silva, F. Cercas, and M. Tomlinson, "Iterative fde design for ldpc-coded magnitude modulation schemes," in *Wireless Communication Systems (ISWCS 2013), Proceedings of the Tenth International Symposium on*, Aug 2013, pp. 1–5.

[16] S. Lin and J. D. J. Costello, *Error Control Coding, 2nd ed.* NJ: Pearson Prentice Hall, 2004.

[17] R. Dinis, A. Gusmão, and N. Esteves, "On broadband block transmission over strongly frequency-selective fading channels," in *IEEE Wireless'03*, Calgary, Canada, July 2003.

[18] N. Benvanuto and G. Cherubini, *Algorithms for Communications Systems and Their Applications*. Chichester, U.K.: Wiley, 2002.

[19] A. Gusmão, R. Dinis, and N. Esteves, "On frequency-domain equalization and diversity combining for broadband communications," *IEEE Trans. Commun.*, vol. 51, pp. 1029–1033, July 2003.